Resting-state test–retest reliability of a priori defined canonical networks over different preprocessing steps

Deepthi P. Varikuti, [1,2,*]

Phone +49-2461-61-96411
Email d.varikuti@fz-juelich.de

Felix Hoffstaedter, [1,2]

Sarah Genon, [1,2]

Holger Schwender, [3]

Andrew T. Reid, [2]

Simon B. Eickhoff, [1,2]

[1] Institute of Clinical Neuroscience and Medical Psychology, Medical Faculty, Heinrich Heine University Düsseldorf, Düsseldorf, Germany

[2] Institute of Neuroscience and Medicine (INM-1), Research Center Juelich, 52425 Juelich, Germany

[3] Mathematical Institute, Heinrich Heine University Düsseldorf, 40225 Düsseldorf, Germany

Abstract

Resting-state functional connectivity analysis has become a widely used method for the investigation of human brain connectivity and pathology. The measurement of neuronal activity by functional MRI, however, is impeded by various nuisance signals that reduce the stability of functional connectivity. Several methods exist to address this predicament, but little consensus has yet been reached on the most appropriate approach. Given the crucial importance of reliability for the development of clinical applications, we here investigated the effect of various confound removal approaches on the test–retest reliability of functional-connectivity estimates in two previously defined functional brain networks. Our results showed that gray matter masking improved the reliability of connectivity estimates, whereas denoising based on principal components analysis reduced it. We additionally observed that refraining from using any correction for global signals provided the best test–retest reliability, but failed to reproduce anti-correlations between what have been previously described as antagonistic networks. This suggests that improved reliability can come at the expense of potentially poorer biological validity. Consistent with this, we observed that reliability was proportional to the retained variance, which presumably included structured noise, such as reliable nuisance signals (for instance, noise induced by cardiac processes). We conclude that compromises are necessary between maximizing test–retest reliability and removing variance that may be attributable to non-neuronal sources.

Keywords

Test–retest
fMRI
Resting-state functional connectivity
Reliability
Confound removal

Electronic supplementary material

The online version of this article (doi:10.1007/s00429-016-1286-x) contains supplementary material, which is available to authorized users.

Introduction

Functional magnetic resonance imaging (fMRI) relies on the measurement of changes in blood oxygenation (i.e., BOLD) and plays a vital role in understanding normal and abnormal brain functioning. For instance, functional connectivity of distant brain regions can be investigated through the statistical analysis of coherent low-frequency BOLD fluctuations. Synchronized signal fluctuations can be observed even when the subject is at rest, without performing any task, and the analysis of resting-state data has become a popular means of studying ongoing brain activations and functional connectivity between brain regions (Biswal et al. 1995; Fox and Raichle 2007). There are both indirect (from comparison with task co-activation patterns, (Kwong et al. 1992; Hinke et al. 1993; Buckner et al. 1996; Huettel et al. 2004; Barch et al. 2013)) and direct (from invasive recordings (He et al. 1999; Lai et al. 2011; Lu et al. 2014) supports toward this notion. Several confounding effects, including system noise, thermal noise, and noise induced by non-neuronal physiological processes, may influence the measured signal and hence apparent brain activity. Therefore, interpretation of brain activity depends on the ability to mitigate their influences (Fox et al. 2009).

Participant-induced artifacts, such as motion and physiologically induced artifacts (i.e., due to respiration and cardiac processes), comprise the largest component of noise affecting the BOLD signal (Windischberger et al. 2002). Motion artifacts have been shown to produce spurious correlations in a systematic way (Van Dijk et al. 2012; Power et al. 2012; Satterthwaite et al. 2013), implying that the removal of motion related artifacts is a prerequisite for further analysis. Various approaches have been proposed for dealing with noise effects post hoc, i.e., after the data have been acquired (Behzadi et al. 2007; Fox et al. 2009; Murphy et al. 2009; Chai et al. 2012; Griffanti et al. 2014; Patriat et al. 2015; Power et al. 2015; Soltysik et al. 2015; Wong et al. 2016). In addition to motion-related artifacts, one particular aspect that has received a lot of attention is the use of nuisance regressors reflecting global signals, derived either from the whole brain or from specific tissue types, such as white-matter or cerebrospinal fluid. However, removal of various global nuisance regressors alters the variance of the residual signal and has been shown to modify the correlational structure (Fox et al. 2009). In line with it, Friston (2011) showed that changing the signal-to-noise ratio can change the correlation coefficient, which indicates that the level of observable noise influences the correlation coefficient.

Both the definition of the ROI from which BOLD signals are extracted and the means by which voxel-wise signals are summarized across a given ROI are critical considerations in a functional connectivity analysis. An ROI can be derived through various approaches, including (most simply) a single voxel or sphere of a fixed radius around a voxel, histological parcellation in standard space (Eickhoff et al. 2005), clustering approaches based on functional or structural connectivity estimates (Eickhoff et al. 2015), thresholded statistical maps, or meta-analytic approaches such as ALE (Eickhoff et al. 2009, 2012). In this study, we focused on region-to-region connectivity within a priori meta-analytically defined networks (Schilbach et al. 2014; Schilbach 2016). This approach has several advantages. In particular, meta-analyses provide robust, functionally specific ROIs based on observations across many studies. Analyzing functional connectivity on this network combines its functional specificity with the advantages of task-free imaging, i.e., an acquisition that poses little demands on the subjects and is not confounded by a specific task paradigm. Similarly, the extraction of a summary signal across an ROI can be performed in various ways that may impact the reliability of connectivity estimates. In particular, the exclusion of voxels based on their gray matter probabilities may help improve signal to noise by removing signal not originating in the gray matter tissue of interest. In this study, we compared three signal extraction approaches using different gray matter masking techniques.

Many clinical studies currently rely on functional connectivity measures in understanding normal and abnormal brain functioning. The appeal for resting-state functional connectivity analyses in clinical applications lies in the fact that such data are easy to acquire without any specific setup, do not require active participation by the subjects, and in contrast to task-based data, are less influenced by compliance and performance. Nevertheless, several concerns have been raised regarding the reproducibility and statistical power of classical neuroimaging studies (Button et al. 2013a, b). Clinical application, however, can only be useful if the analyses yield reliable measures. Various studies have also been performed to test the reliability of functional or effective connectivity measures using different modalities (such as fMRI or diffusion MRI) and reported moderate to high test–retest reliability of connectivity measures across moderate to long-term scans. (Chen et al. 2015; Frässle et al. 2016; Song et al. 2016; Zhong et al. 2015). Shehzad et al. (2009) investigated the test–retest reliability of global connectivity patterns using resting-state fMRI and observed that significant connectivity scores are more reliable than non-significant connectivity scores. Wang et al. (2011) evaluated short-term (less than 1 h apart) and long-term (more than 5 months apart) test–retest reliability for topological metrics of functional networks and observed that long-term scans had better reliability than short-term scans. Later, Raemaekers et al. (2012) analyzed the reliability of BOLD activation and reported that patterns of BOLD activation were relatively stable across sessions, while the amplitude of the activations is more variable. Gorgolewski et al. (2013) studied the test–retest reliability of confound removal at the subject level (by focusing on the single subject reliability) and showed that subject motion can detrimentally impact reliability. Yan et al. (2013b) investigated the influence of post-acquisition standardization techniques on traditional fMRI measures, test–retest reliability, and phenotypic relationships, as well as nuisance variables (mainly mean global signal) and reported that global signal regression is identical to gray matter regression and both should be avoided. Subsequently, Birn et al. (2014) evaluated the influence of various physiological noise correction methods on test–retest reliability and found that it was reduced by physiological noise correction, as it reduced the variability between subjects as well as within the subject. Shirer et al. (2015) investigated various means of confound removal across multiple outcome measures and demonstrated that noisiness, reliability, and heterogeneity of the data varies based on the preprocessing parameter chosen. In turn, the influence of various gray matter masking approaches on the reliability has not been addressed in any of the previous test–retest studies. Therefore, using meta-analytically derived networks, we assessed the influence of different signal extraction and noise regression approaches on the reliability of the resting-state functional connectivity measures.

In this study, we evaluated test–retest reliability of resting-state functional connectivity in a cohort of 42 subjects scanned twice with a between-scan interval of 175 ± 75 days. We assessed two networks: the extended socio-affective default mode network (eSAD) (Amft et al. 2015); and the working-memory network (WMN) (Rottschy et al. 2012). Both networks were derived from previous meta-analytic studies, which used anatomical likelihood estimation (ALE; (Eickhoff et al. 2009, 2012)) to identify regions that are robustly activated across studies, for specific task paradigms. Both networks have been hypothesized to anti-correlate with each other (Fox et al. 2005; Reid et al. 2016). Thus, the reliability of connectivity estimates within, as well as between, the specified meta-analytically derived networks was evaluated.

A literature survey was conducted, to investigate the popularity of various methods for confound removal in recent fMRI studies. Using PubMed database, all the articles with the terms “fMRI,” “resting-state,” and “seed-based,” published from the beginning of 2014 until the time of this study (June 2016) were identified, reflecting the recent work most in line with the focus of our work on seed-based analyses. A total number of 239 studies were identified. Among them, 33 studies had to be excluded, because the articles were either not relevant to the study (such as studies on animals) or not accessible. Therefore, a total number of 206 studies were investigated. We then computed the percentage of studies using the different confounds removal methods, which is shown in Fig. 1 . The frequency of studies when using a certain confound has been demonstrated separately (in the categories of ‘Only’) and in combination with the other confounds in the Fig. 1 .

Fig. 1

Percentage of studies using a certain confound removal method [i.e., white matter and cerebral spinal fluid signal regression (WMCSF), global signal regression (GSR), principle component analysis-based corrections (PCA), tissue signal regression (TSR), physiological recordings-based corrections (physiological correction), independent component analysis-based corrections (ICA), and other correction methods such as ANATICOR or gray matter atrophy regression (others)]. The *colors* represent the interactions of each method with other methods. The first fraction of section which is consistent over the approaches, represented with the word “Only” (in *blue*) shows the percentage of studies performing only a certain confound removal without any interactions. Additional colors assigned to the other confound removal appears only when there is an interaction. Of note, the interactions of motion regression with other methods are not explicitly shown in this figure. However, almost all the studies involved in this literature survey have removed the motion effects along with the other confound removal approaches demonstrated in the figure

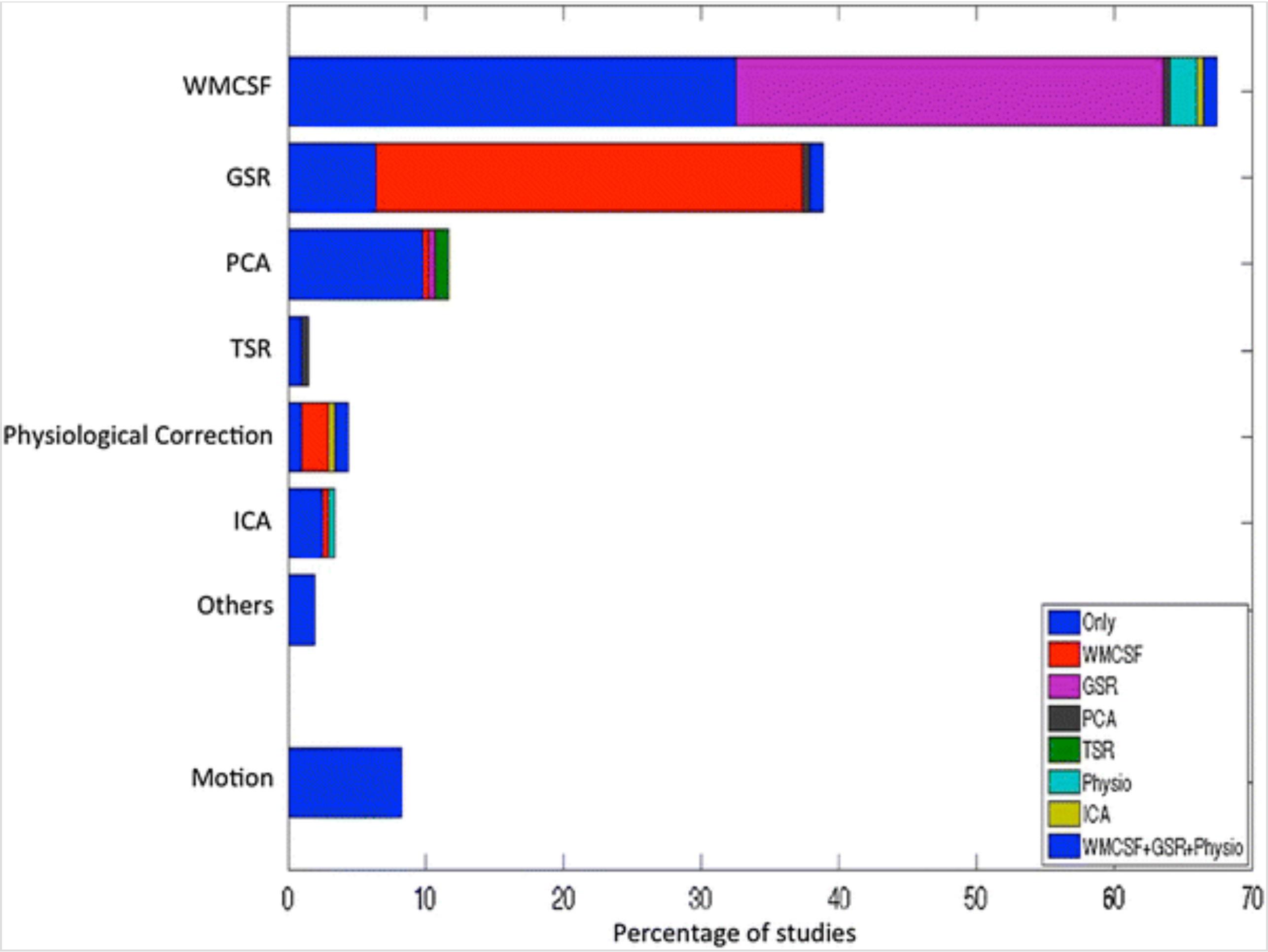

AQ1

Based on this literature examination, we assessed the effects of the most commonly used confound removal approaches in resting state fMRI studies; namely, global and tissue-class specific (either only WM and CSF or in addition also GM) mean signal regression, as well as principal components analysis (PCA) denoising. We also examined three approaches for extracting the regional time-series based on different methods for gray matter masking. Above mentioned approaches were assessed separately and in combination with each other. To observe the consequences of the interactions, the approaches were evaluated in combinations (cf. "Assessed (combinations of) signal processing steps"). We note that physiological noise regression (i.e., elimination of artifacts induced by respiration and cardiac processes) requires recordings of parameters, such as heartbeat and breathing. Such physiological recordings, however, are rarely acquired in standard (clinical) resting-state acquisitions and were hence not considered in the current investigation. Independent component analysis (ICA)-based denoising is another emerging approach to confound removal (Griffanti et al. 2014; Salimi-Khorshidi et al. 2014; Pruim et al.

2015a, b). However, ICA-based denoising approaches (excluding the ICA-AROMA, as the pre-defined spatial features included within in the package itself) require effective individual segmentation from high-resolution T1 images, which were not available for the current data. Acknowledging the future potential of ICA-based denoising, we thus focused our work on the evaluation of the presently most widely used approaches.

Another common application of ICA is the examination of the functional connectivity networks. Recently, such ICA method followed with the dual regression is used to assess the functional connectivity for group comparisons, instead of seed-based functional connectivity. Zuo et al. (2010) reported moderate-to-high test–retest reliability. Furthermore, Smith et al. (2014) claimed that ICA followed with the dual regression performs better than the seed-based connectivity measures. Even though, such methods may lead to higher reliability. Zuo et al. (2010) reported moderate-to-high test–retest reliability, while computing the functional connectivity networks using ICA combined with the dual regression. Furthermore, Smith et al. (2014) investigated that ICA followed with the dual regression performs better than the seed-based connectivity measures. Even though such methods may lead to higher reliability (Zuo et al. 2010), seed-based functional connectivity is still very widely used for the examination of a priori hypotheses in both basic and clinical studies (Smith et al. 2014). Thus, we here focused on the test–retest reliability of the seed-based functional connectivity measures.

Importantly, reliability can be examined from two perspectives: at the subject level and at the connection level. One the one hand, meaningful group comparisons largely depend on reliability at the subject level, i.e., over scans the order of subjects should remain as similar as possible for any given connection. One the other hand, network modeling capitalizing on within-subject connectivity requires reliability at the connection level (cf. “Indices of reliability”), i.e., for any given subjects, the order of connectivity strengths should remain as similar as possible over scans. Therefore, in this study, we investigated reliability from the two different but complementary perspectives, that is, reliability at the subject level (RoSO) and reliability at the connection level (RoCO). To sum up, this study aimed to identify the combination of signal extraction and confound removal approaches that yield the highest test–retest reliability when assessing resting-state functional connectivity in meta-analytically defined networks, using standard acquisitions as feasible in clinical practice. In other words, this study aims to provide a ranking of methods in terms of their potential to yield stable connectivity patterns over time.

Materials and methods

Networks of interest

The influence of different processing steps on the test–retest reliability of resting-state functional connectivity analyses was assessed in two canonical networks related to cognitive and socio-affective processing. In particular, the two networks were defined by large-scale synthesis of neuroimaging findings using coordinate-based meta-analyses (Fox et al. 2014). As a prototypical “task-positive” cognitive network (regions exhibiting increase in activity during task performance), we assessed the core working memory network (WMN) described by Rottschy et al. (2012), consisting of nine bilateral fronto-parietal regions (Fig. 2a; Table 1). As a “task-negative” network (regions exhibiting decrease in activity during task performance), we included the extended socio-affective default mode (eSAD) network identified by Amft et al. (2015), which extended a previous meta-analytical definition of the default mode (Schilbach et al. 2012) and comprised 12 regions mainly corresponding to cortical midline structures (Fig. 2b; Table 1). Importantly, both of these networks have shown a strong positive coupling among their respective nodes but were anti-correlated with each other. They may thus be considered as robustly a priori defined network models for the often-proposed large-scale anti-correlated systems in the human brain (Fox et al. 2005).

Fig. 2

Nodes of meta-analytically derived networks used for the reliability assessment. **a** The core working memory network (Rottschy et al. 2012). **b** The extended socio-affective default mode network (Amft et al. 2015)

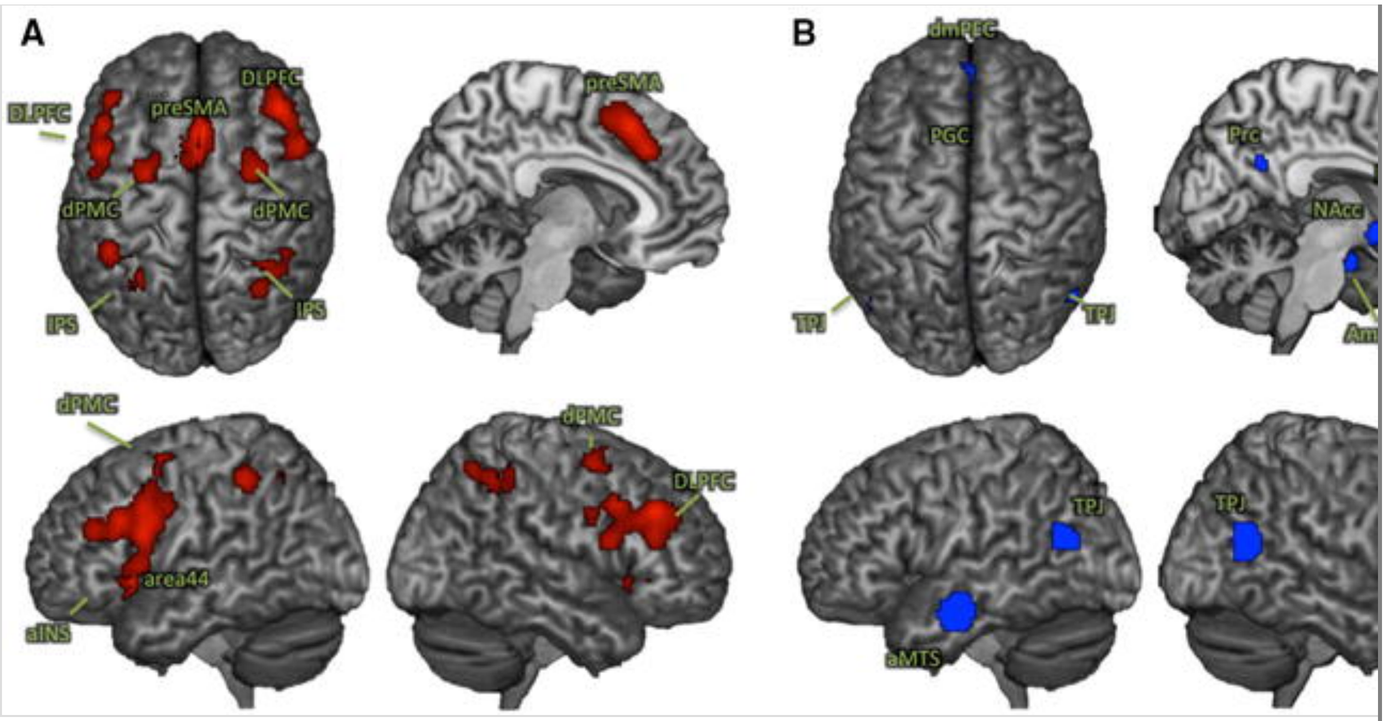

Table 1

Coordinate details and cluster size (*k*) of the regions, within the WMN and eSAD inv in this study

	Macro-anatomical labels	**Abbreviation**	**Side**	***k* (voxels of size 3.1 mm isotropic)**	**MNI coordinat in standard R orientation**		
					X	***Y***	***Z***
Working memory network (WMN) nodes							
1	Anterior insula	aINS	L	276	32	22	−
2			R	182	34	28	−
3	Dorsolateral prefrontal cortex	DLPFC	L	1331	50	12	2
4			R	1032	44	34	3
5	Pre-supplementary motor area	preSMA		1035	2	20	5
6	Intraparietal sulcus	IPS	L	543	30	56	4
7			R	310	36	48	4
8	Dorsal premotor cortex	dPMC	L	190	28	0	5
9			R	243	30	2	5

Extended socio-affective default mode (eSAD) network nodes							
10	Pregenual anterior cingulate cortex	ACC		180	0	36	1
11	Anterior middle temporal sulcus	aMTS	L	468	54	10	−
12	Amygdala/hippocampus	Amy/hippo	L	86	24.0	10	−
13			R	141	24	−8.0	−
14	Basal ganglia	BG	L	146	−6	10	−
15			R	188	6	10	−
16	Dorsomedial prefrontal cortex	dmPFC		204	−2	52	1
17	Precuneus	PrC		145	−2	52	2
18	Subgenual anterior cingulate cortex	sACC		244	−2	32	−
19	Temporo-parietal junction	TPJ	L	251	46	66	1
20			R	373	50	60	1
21	Ventromedial prefrontal cortex	vmPFC		114	−2	50	−

Sample characteristics, preprocessing and RS-FC computation

Images acquisition

Resting-state fMRI data of 42 healthy subjects including 19 females with an average age of 42 ± 20 (mean ± std) years were obtained in two sessions with an average time interval of 175 ± 75 (mean ± std) days. In each session, 250 resting state EPI images were obtained on a Siemens 3T Scanner (Scanning parameters: TR 2200 ms, TE 30 ms, flip angle 90°, 36 slices, a voxel size 3.1 mm isotropic) corresponding to a scanning time of 9.2 min, which stays well in line with the reliable intersession scanning time of 8–12 min suggested by Birn et al. (2013). High-resolution T1-weighted structural images were not acquired for the data set used in this study. The original study protocol of the data used here has been approved by the local ethics committees of the university hospital Aachen, and informed consent was obtained by all the participants prior to the examination. The current data were analyzed anonymously.

Images preprocessing

Prior to further processing (using SPM8, http://www.fil.ion.ucl.ac.uk/spm), the first four images were discarded allowing for magnetic field saturation. The EPI images were corrected for head movement by affine registration using a two-pass procedure. In a two-pass procedure, all the EPI images were aligned to the first EPI image. Then, a mean over the aligned EPI images was computed. Finally, all the EPI images were again aligned to the first pass mean EPI image. The mean EPI image for each subject was non-linearly normalized to the MNI152 non-linear template space template using the “unified segmentation” approach (Ashburner and Friston 2005). The ensuing deformation field was applied to the individual EPI volumes and smoothed with a 5-mm FWHM Gaussian kernel. Preprocessed images were visually checked for any processing artifacts.

Each node of the assessed functionally defined networks (cf. “Networks of interest”) available in the same space was represented by its peak’s coordinate. The time series for all voxels within a priori meta-analytically derived clusters were then extracted. Following gray matter masking if applicable (cf. “Assessed (combinations of) signal processing steps”), we then employed a multiple regression approach to control for different confounds in the EPI time series. While the choices for dealing with global signals were outlined below, we always included the six motion parameters derived from the image realignment as well as their derivative as the first-order (linear) and second-order (quadratic) terms as evaluated by (Satterthwaite et al. 2013). That is, in addition to the approach-specific confounds, these 24 movement regressors were used in all analyses. Following the removal of any variance in the individual voxels’ time series that could be explained by the respective confounds, the data were band pass filtered preserving BOLD frequencies between 0.01 and 0.08 Hz (Biswal et al. 1995; Fox and Raichle 2007). We computed the frame-to-frame differences from the six motion parameters derived from the image realignment to assess frame-wise displacements (FD).

An FD threshold of 0.5 mm was used to discard potentially motion-contaminated images, before bandpass filtering (Power et al. 2012; Yan et al. 2013a). Finally, the characteristic time series of each seed was computed as the first eigenvariate of the preprocessed time series for the individual voxels within that seed. The functional connectivity between every pair of nodes was then computed as the correlation coefficient between these time series, which were transformed to Fischer's *Z* scores to render them normally distributed (Fig. 3). Here, in this study, tissue class segmentation is performed on a mean EPI volume due to the lack of high-resolution T1 structural scans. Nevertheless, the registration of EPI images to T1 structural scans may fail to detect the non-linear distortions of the EPI images, especially in the absence of the field maps or such relevant images. However, partial volume effects may exist in the mean EPI volume based segmentation. To avoid such partial volume effects, gray matter masking along with a median-split approach, which extracts the signal only from 50 % of the voxels with high gray matter probability, has been implemented and evaluated in this study. In addition, median-split approach has an advantage of accounting similar number of voxels while extracting the signal, particularly when using meta-analytically derived clusters.

Fig. 3

Pipeline of the entire preprocessing steps until the RS-FC computation: the assessed combinations (inside the *red dotted box*) indicate the signal processing methods for which the reliability is evaluated in three different domains ((I) extraction of time series, (II) PCA denoising, (III) global signal removal)

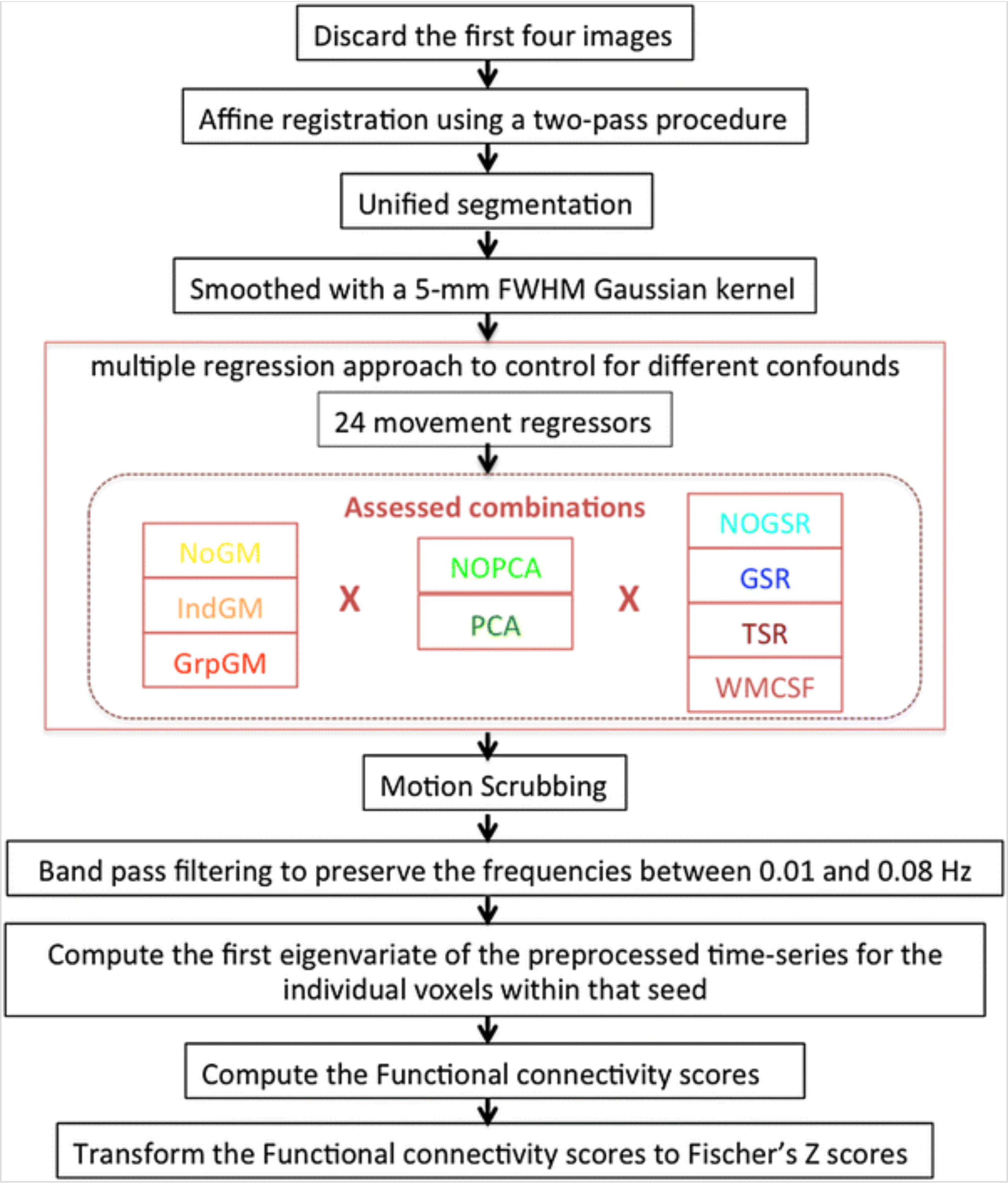

Assessed (combinations of) signal processing steps

As the key aim of this study was to assess the impact of different commonly used processing steps on the reliability of RS-FC measurements, we focused on three different domains as follows.

AQ2

(I) Extraction of time series: Evidently, meaningful signal should mainly be found in gray matter (GM). Hence, the voxels within 5 mm of the seed's coordinate might be anatomically constrained based on tissue class segmentation as provided by SPM (Ashburner and Friston 2005). Here, we evaluated three options:

No gray matter mask (*NoGM*) All voxels within 5 mm of the seed coordinate were included, processed by confound removal and temporal filtering, and summarized by their first eigenvariate. No gray matter masking is the most commonly used approach in RS-FC analysis. Conceptually, NoGM considered the influence of cortical anatomy as minor relative to the spread of BOLD data and spatial smoothing.

Individual gray matter mask (*IndGM*) The GM probability as estimated by the unified segmentation for that particular subject was extracted for each voxel within 5 mm of the seed coordinate and a median-split approach was then performed retaining those 50 % of voxels with highest GM probabilities. This approach was based on the argument that the individual anatomy should be most important for tissue classification.

Group gray matter mask (*GrpGM*) The tissue class segmentations of all individual subjects were first averaged and a median-split approach of the voxels was then performed based on these average GM probabilities. In this method, the focus on GM was retained but rather than basing the masking on the (prominently noisy) individual segmentation, group data (considered as more robust) were used. For reader's information, the overlap between the *IndGM* and *GrpGM* was computed and is shown in Fig. 4.

Fig. 4

Percentage of voxels that overlap between the individual and group masks, relative to the *GrpGM* for each of the 21 seed regions

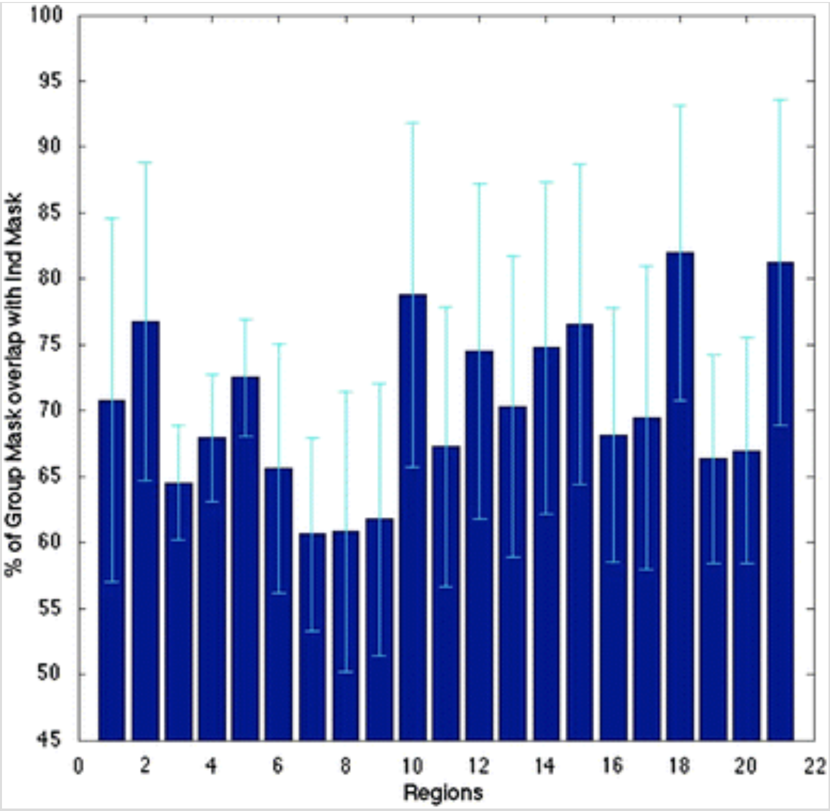

(II) PCA denoising: It has been suggested (Behzadi et al. 2007; Soltysik et al. 2015) that computing a principal component analysis (PCA) decomposition across the WM and CSF regions of the brain and removing variance associated with the most dominant five components might remove many sources of artificial and confounding signals and hence increase the specificity of RS-FC results. We thus performed all analyses both with (PCA) and without (NoPCA) PCA denoising.

(III) Global signal removal: As removing the global signal had received a lot of attention in recent discussions (Murphy et al. 2009; Chai et al. 2012; Saad et al. 2012; Fox et al. 2013), we assessed seven different methods for this particular aspect. In that context, tissue class-specific global signals were computed based on the SPM8 segmentation of the (mean) EPI into GM, WM, and CSF regions, then averaged the signal time series of the voxels specific to each tissue class.

Global signal regression (*GSR*) Removes all variance explained by the first-order effects of the global (average across all voxels at each time point) signal.

Tissue signal regression (*TSR*) Removes variance explained by the first-order effects of the mean GM, WM, and CSF signals.

WM and CSF signal regression (*WMCSF*) The mean signals of the WM and CSF were removed, i.e., only the first-order effects.

No global signal regression (*NoGSR*) No removal of any global signal.

Importantly, the different choices for each of the three main factors may be implemented independently of the other factors, allowing for a full permutation of the different analyses options and hence 42 (3 × 2 × 7) different combinations for signal extraction and confound removal. We, therefore, performed reliability analysis for all of these 42 combinations, i.e., analytical approaches.

Indices of reliability

To quantify the test–retest reliability of the 42 different approaches, we used two complementary measures that were each applied from two different perspectives. Test–retest reliabilities are quite often assessed using intra-class correlations (ICC), which takes into account inter-subjects variability in relation with the intra-subject variability. The intention of our study, however, was to examine one effect at a time, i.e., to evaluate inter-subject variability (i.e., RoSO) separately from intra-subject variability (i.e., RoCO). Therefore, reliability was tested using two measures. The first employed measure was Kendall's rank correlation (to quantify the consistency in relative order; Zang et al. 2004; Shehzad et al. 2009; Guo et al. 2011; Thomason et al. 2011; Li et al. 2012; Patriat et al. 2013) between the functional connectivity scores obtained at the first and second sessions, which quantifies the degree to which the order of observations is similar across both sessions. Modifications in the signal extraction and confound removal methods alter the residual signal fluctuations, which lead to variation in the connectivity measures. Thus, the stability of the relative orders when comparing different connections/subjects was measured using Kendall's correlations. Complementing this index, we computed the absolute difference between functional connectivity scores to probe the numerical test–retest reliability. This index should be less sensitive to single outliers, in comparison with other alternatives like sum of squared measures. Thus, numerical differences when comparing different connections/subjects were measured using mean absolute differences.

These indices were computed from two different perspectives, reflecting the reliability at the subject level and at the connection level, respectively. In that context, reliability at the connection level (RoCO) addresses the question “are, for a given subject, the connections in the same order across sessions?” which was a prerequisite for any within-subject network modeling. We thus computed for each subject the correlation (across connections) between the first and second sessions (Fig. 5 a) as well as the absolute difference between the two sessions by averaging them over connections (Fig. 5 c). This perspective thus yields for every approach as many data points as there were subjects’ within/between the two networks. Reliability at the subject level (RoSO) addresses the question “are, for a given connection, the subjects in the same order across sessions?” which was a prerequisite for group comparisons. Here, we computed for each connection the correlation (across subjects) between the first and second sessions (Fig. 5 b) as well as the absolute differences between the two sessions by averaging them over subjects (Fig. 5 d). This perspective thus yields, for every approach, the same number of data points, as there are connections in the respective network.

Fig. 5

Indices of the reliability: the four indices of reliability used here are shown. **a**, **b** Functional connectivity at two time points (**a**) at connection level, i.e., for all connections within a given subject (**b**) at subject level, i.e., for all the subjects within a given connection [here between left and right anterior insula (LaIns–RaIns)]. **c**, **d** Absolute differences of functional connectivity scores between the two sessions (**c**) at the connection level, i.e., the mean of the absolute differences over subjects for the 210 connections, and **d** at the subject level, i.e., the mean of the absolute differences over connections for the 42 subjects. **e** The variance within the BOLD signal time series of the left anterior Insula for two different combinations of signal processing methods [“GrpGM NoPCA NoGSR” (*black*), “NoGM PCA TSR” (*red*)]

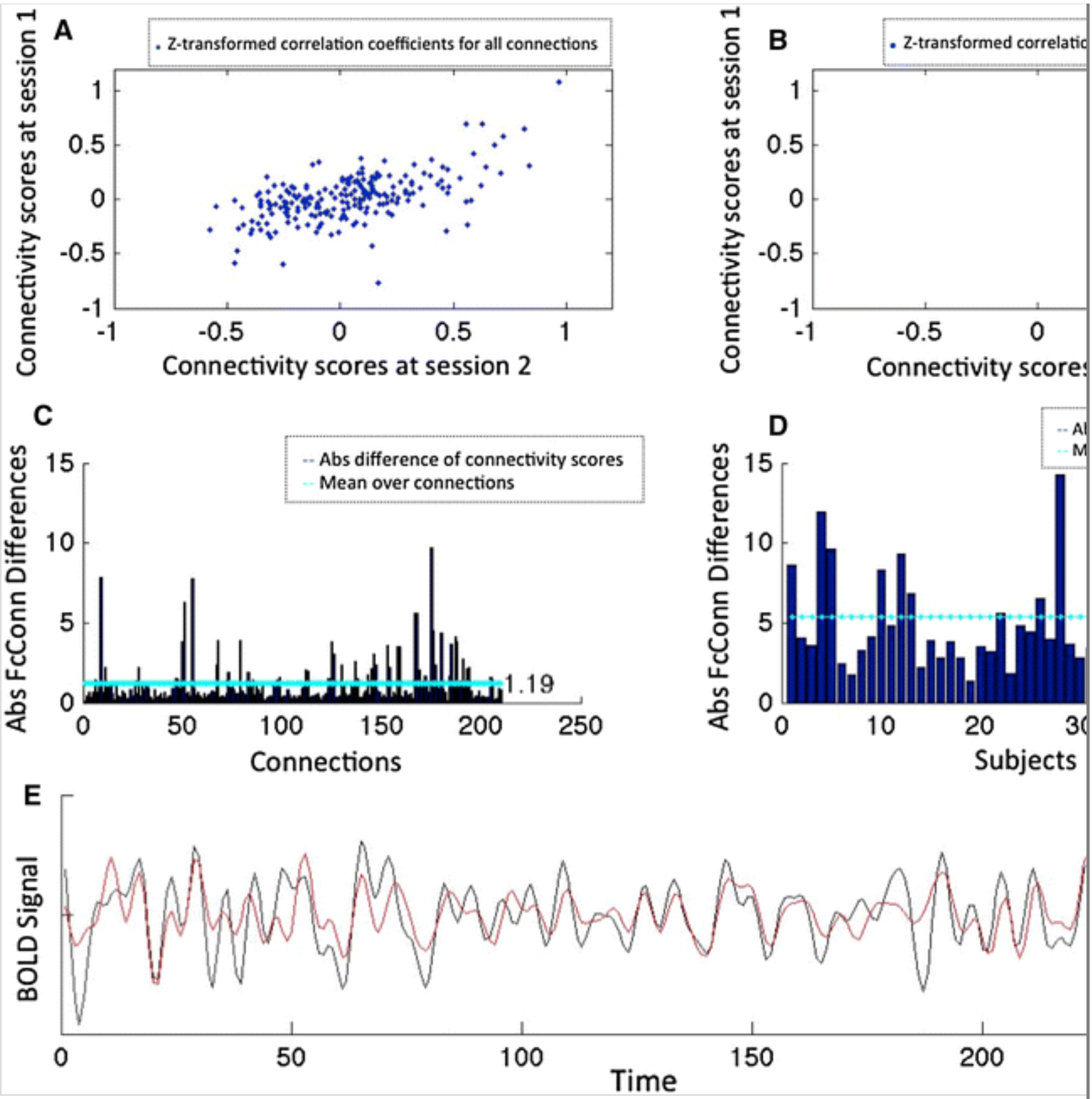

Finally, we computed two further important parameters in addition to these indices of reliability. First, the amount of variance within the extracted time series at the two time points was computed for each combination of methods to quantify the influence of confound removal on the variance of the residual resting-state signal (Fig. 5 e). Second, for every approach, we computed percentage of positive connectivity scores among within-network (i.e., within eSAD and WMN regions) and between-network connections (i.e., between eSAD and WMN regions).

Aggregation and evaluation

The 42 different approaches defined by the combination of different masking/confound removal approaches were compared using a non-parametric Friedman ANOVA for each of the assessed parameters (correlations and absolute differences, each assessed at subject and connection level (Supplementary figures S5–S7), as well as residual variance in the time series). To aggregate these findings, the individual approaches were ranked according to their reliability scores for each parameter. Subsequently, these reliability ranks were added over the different perspectives to obtain an overall reliability ranking. The overall reliability ranks allowed to identify reliable combination of different confound removal approaches at different perspectives.

Supplementary analysis

Given that the focus of our study was to investigate, which (combination of) analytical choices result in the best test–retest reliability functional connectivity estimates for meta-analytically defined networks, the main analyses used the entire significant clusters of the previously defined eSAD and WM networks as regions of interest (ROIs). Acknowledging the alternative strategy of representing these ROIs by spheres around their center coordinates, we then repeated all analyses using spherical ROIs of 5 mm radius.

Results

The setup of our study allows us to perform a large number of different analyses. We first provide an overview on the test–retest reliability as reflected by the two different measures, i.e., rank-correlations and absolute differences. Here, the rankings based on the reliability of subject order (RoSO) and those based on the reliability of connection order (RoCO) are combined. Next, we present an overview on the reliability from either perspective, combining the two measures. Finally, we provide the overall summary together with the ranking based on the residual variance in the time series as well as the information on the proportion of positive vs. negative connections. The individual test retest rankings by the two different methods and different perspectives are presented in the supplementary results (cf. Supplementary figures S1–S4).

In addition, we would like to note that we present findings for “within-network” and “between-network” connectivity. The former represents a summary of the rankings obtained for the extended socio-affective default mode as well as the working memory network, each showing strong, positive coupling among their respective nodes. The latter represents the connections between all possible pairs of nodes from either of these two major networks that are often conceptualized as being antagonistic to each other.

Reliability using different indices

The combined ranks, based on Kendall’s rank correlations as the measure of subject- and connection-order, are shown in Fig. 6. The approaches are ordered such that the most reliable method is placed on the top, the least reliable on the bottom. It may be noted that for both within- and between-network connections, PCA denoising seems to have a rather detrimental effect on test–retest reliability, as most combinations including PCA denoising rank in the lower half and none is found in the top 10. On the other hand, gray matter masking, which is part of more than half of the ten most reliable approaches, seems to improve reliability. In particular, individual gray matter masking for within-network connections and group gray matter masking for between-network connections provide a better reliability. Global signal removal seems to have detrimental effect on the overall pattern for both within- and between-network connections. No removal again provided the most reliable correlation values for between-network connections. Nevertheless, the rank-order stability of within-network connections was improved by removal of WM and CSF signals (WMCSF).

Fig. 6

Combined rankings of the test–retest reliability at the subject and connection level for Kendall’s correlations and absolute differences. The “within networks” ranking refers to intra-network connections of the working memory and the default mode network and the “between networks” to inter-network connections. The *gray bar* represents the summed ranks for the respective categories

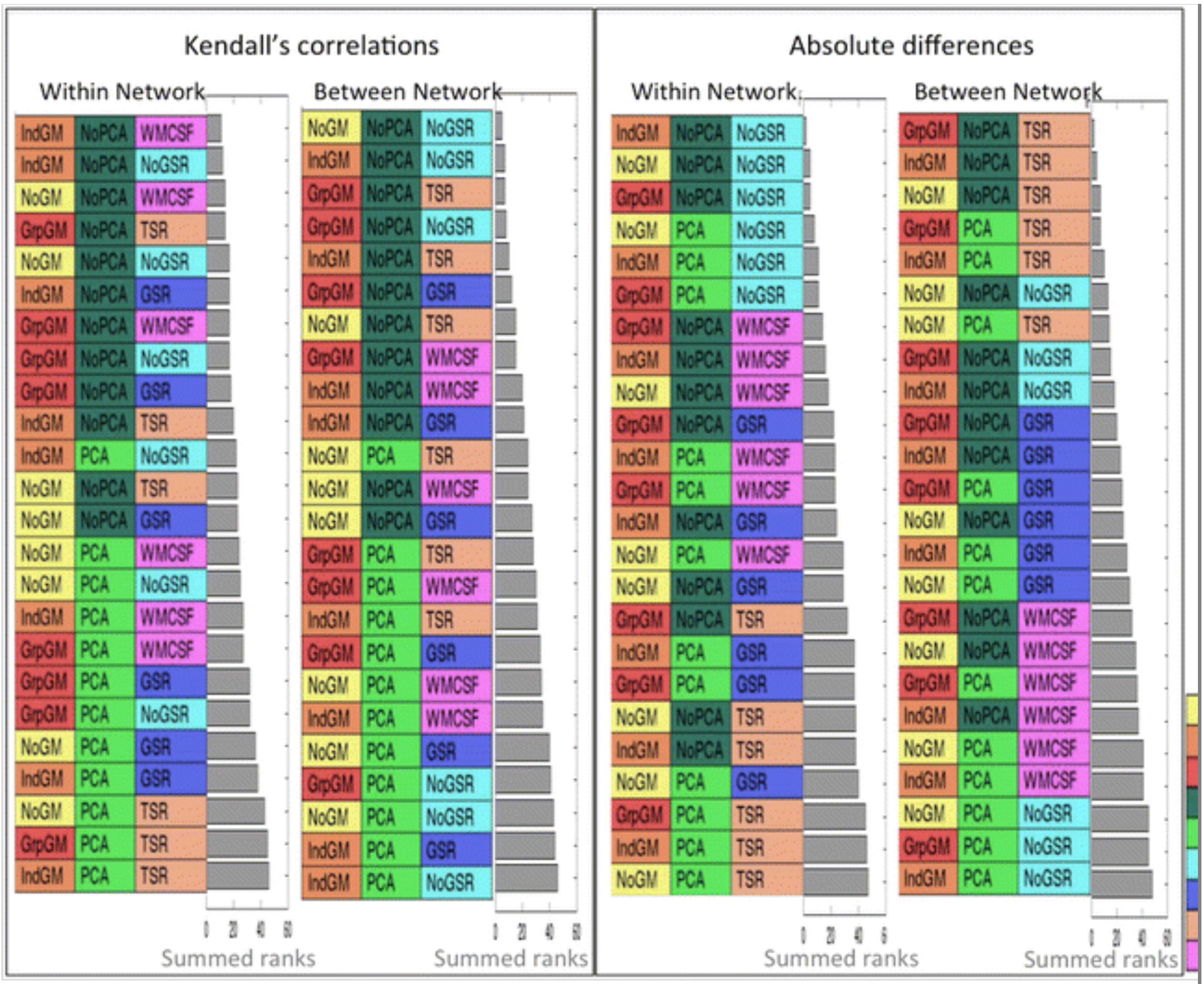

The assessment of reliability, by measuring absolute differences rather than measuring Kendall's correlations, corroborated most of these observations. In particular, we again found that using gray matter masking and refraining from PCA denoising yielded more reliable estimates of functional connectivity. While this pattern is not as clear-cut as for the correlation-based measure, it again held true for both within- and between-network connections. There is, however, a striking change in the overall pattern with respect to the effects of global signal removal. No removal again provided the most reliable absolute values for within-network connections. Nevertheless, the numerical stability of between-network connections was clearly improved by removing the global signal in all three-tissue classes (TSR).

Reliability from the subject and connection perspective

As noted in the methods, RoSO assesses how well the relative differentiation between subjects is reproduced at a second time point and is hence of particular relevance for between-subject analyses, e.g., in clinical application. In contrast, RoCO assesses how well the relative differentiation between connections in a particular subject is reproduced and is hence of particular relevance for within-subject analyses, e.g., in connectome modeling.

Several major trends of reliability noted in the previous section are again well observable in this analysis (Fig. 7). In particular, we again found that PCA denoising has a rather detrimental effect on reliability. In contrast, when considering within-network RoCO, PCA denoising has improved the reliability, namely, in the absence of global signal regression. Moreover, gray matter masking, in particular when using the mean tissue probabilities across the entire group, generally yields more reliable estimates of functional connectivity, although individual gray matter masking is more prominent when considering within-network connections, especially RoCO. With respect to the influence of global signal removal, we again found a more heterogeneous pattern with a clear distinction between within-network and between-network connections. With respect to the former, both RoSO and RoCO are highest when no global signal removal is performed, followed by approaches involving the removal of WM and CSF signals (WMCSF). For between-network connections, linear removal of the global signal for all three-tissue classes (TSR) yields the highest RoSO and RoCO, but for RoCO, neither removing any global signal nor performing a PCA denoising yields the highest reliability with no gray matter masking.

Fig. 7

Summary rankings for RoSO and RoCO. Reliability for within network (WMN and eSAD) and between networks is shown separately each combining Kendall's correlations and absolute difference. The *gray bar* represents the summed ranks for the respective categories

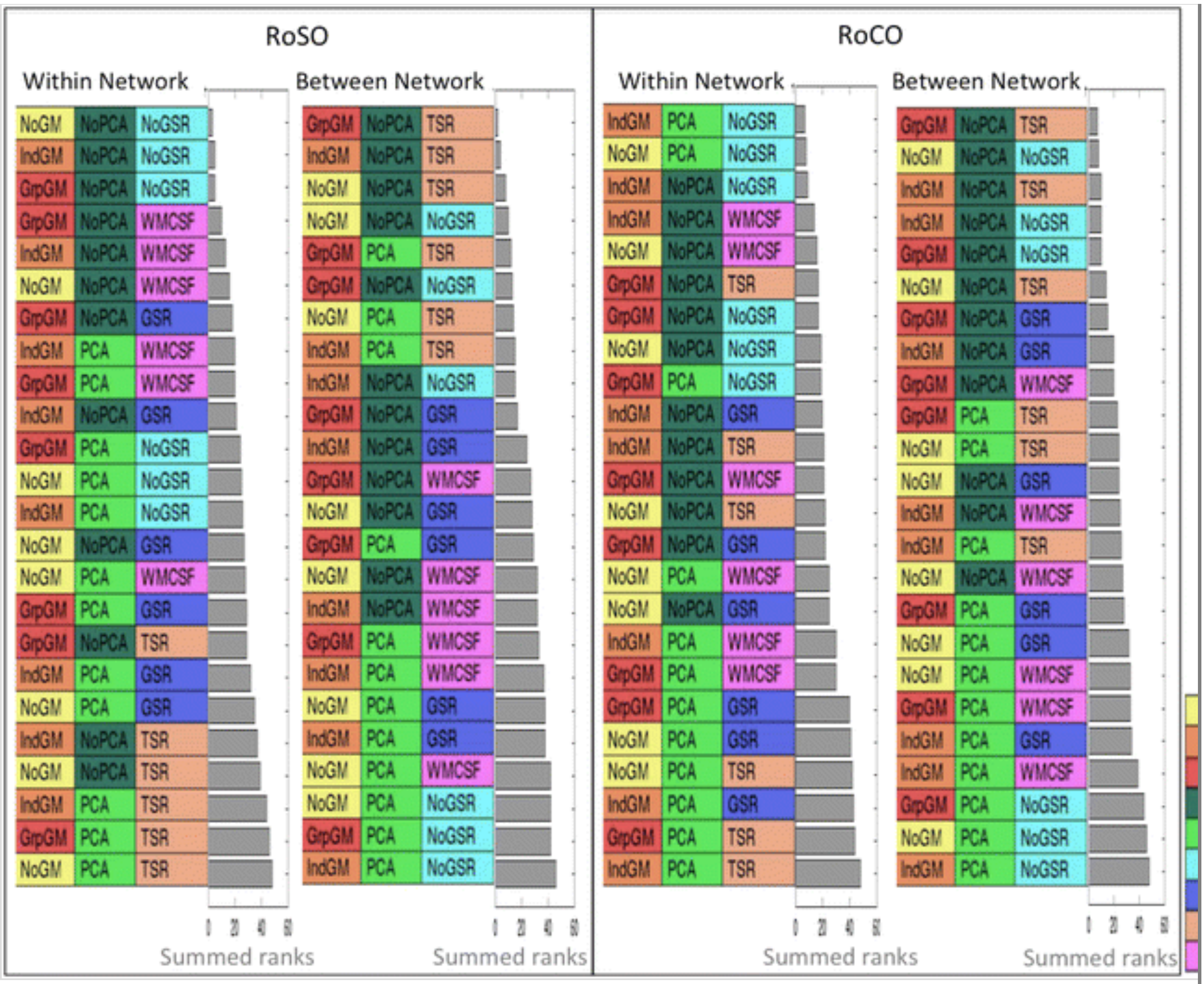

Summary of reliability ranking

The summary ranking across both indices (Kendall's correlations and absolute differences) and both perspectives (RoSO and RoCO) of reliability reflects the major patterns noted in the individual analyses (Fig. 8). Gray matter masking improves reliability. PCA denoising leads to lower test–retest reliability. Within-network connections are most reliably estimated when using no global signal regression and with removing the global WM and CSF signal representing the next-best approach. In contrast, between-network connections are most reliably measured by linear and second-order removal of global signals of all three-tissue classes.

Fig. 8

Summary rankings of reliability across Kendall's correlations and absolute differences as well as RoSO and RoCO, separately for within (WMN and eSAD) and between networks. The *gray bar* represents the summed ranks for the respective categories

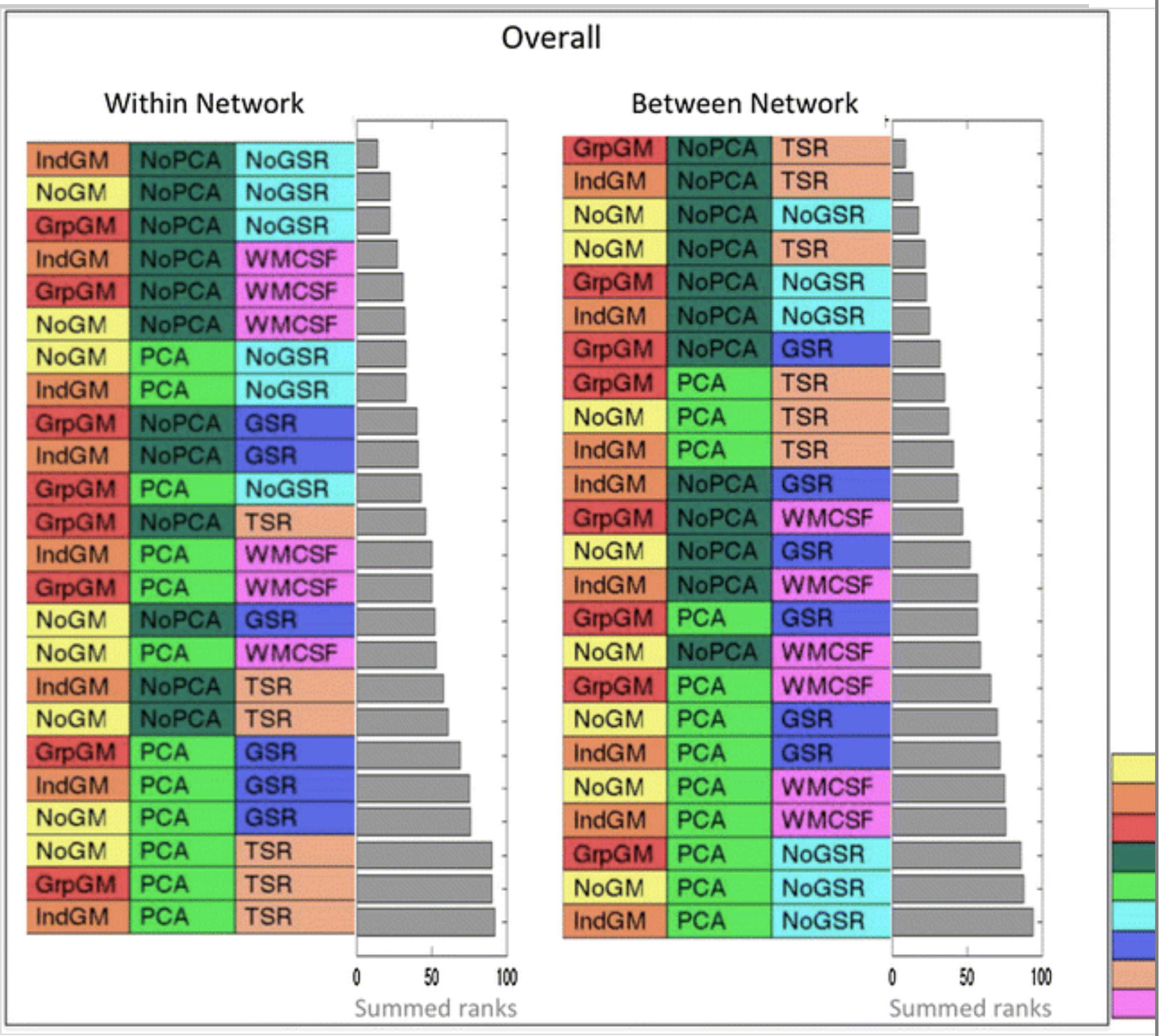

Proportion of positive vs. negative connectivity scores and residual variance in the time series

Addressing the issue of anti-correlations, we assessed the proportion of positive vs. negative connections, i.e., connections with r (and hence Z-scores) below zero (Fig. 9). As expected, within-network connections are predominantly positive. It is, moreover, interesting to note that the least reliable approaches, i.e., those at the bottom of the list, also featured (somewhat) less consistent positive connections. The more striking observation, however, relates to the between-network connections. These are consistently negative when any form of global signal regression is used. If neither global signal regression nor PCA denoising are used, however, all connections are positive. Finally, when PCA denoising but no global signal regression is used, roughly half of the connections are positive.

Fig. 9

The variance left within the time series (far *left column*) and the percentage of positive correlations (*columns* on the far *right*) for both within and between networks arranged by the overall ranking of the reliability. The plots on the *right* side exemplify the difference of the distribution of the connectivity scores at different combinations [“GrpGM NoPCA NoGSR” (*top*), “GrpGM NoPCA WMCSF” (*bottom*)]

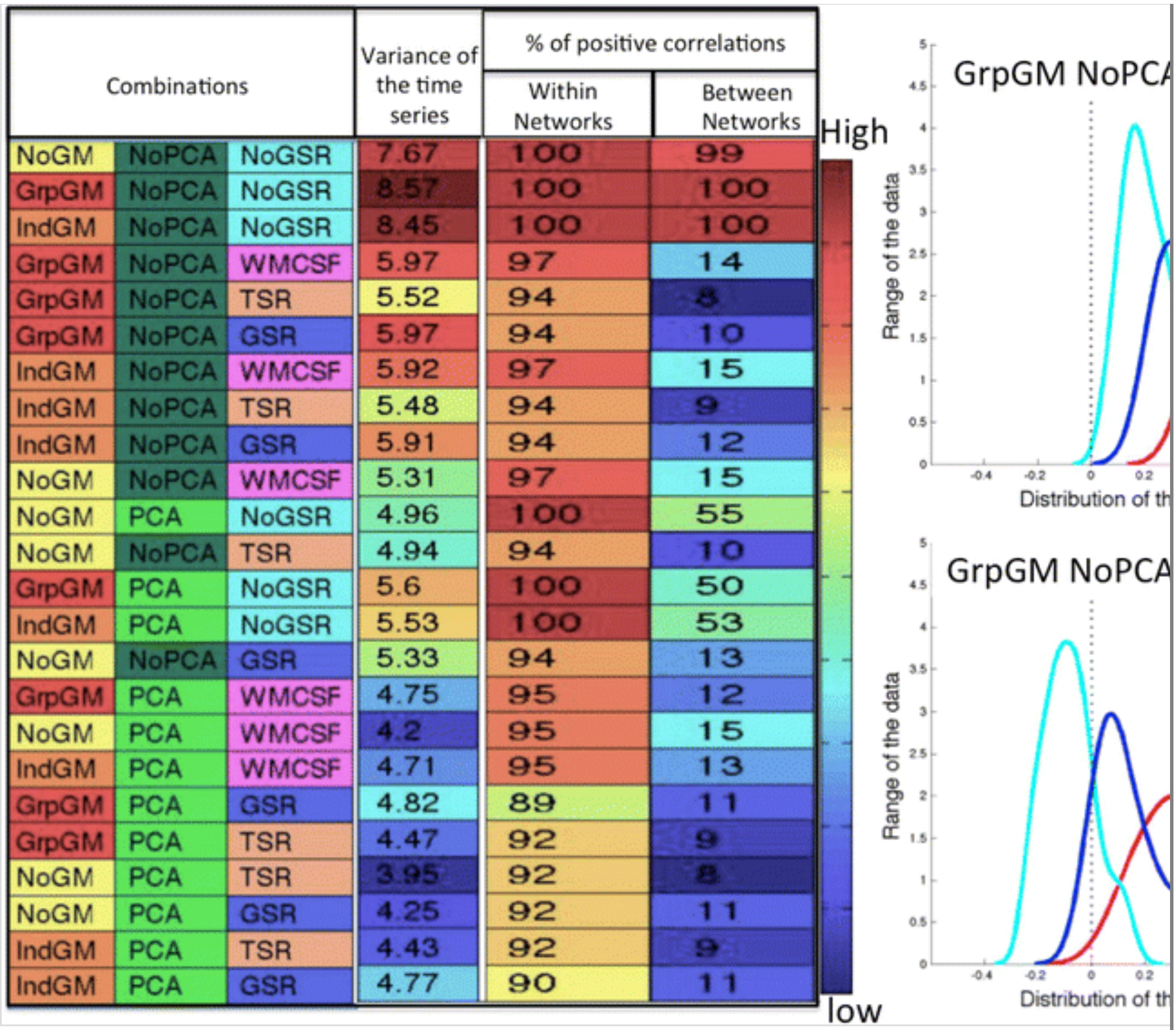

Combinations			Variance of the time series	% of positive correlations	
				Within Networks	Between Networks
NoGM	NoPCA	NoGSR	7.67	100	99
GrpGM	NoPCA	NoGSR	8.57	100	100
IndGM	NoPCA	NoGSR	8.45	100	100
GrpGM	NoPCA	WMCSF	5.97	97	14
GrpGM	NoPCA	TSR	5.52	94	8
GrpGM	NoPCA	GSR	5.97	94	10
IndGM	NoPCA	WMCSF	5.92	97	15
IndGM	NoPCA	TSR	5.48	94	9
IndGM	NoPCA	GSR	5.91	94	12
NoGM	NoPCA	WMCSF	5.31	97	15
NoGM	PCA	NoGSR	4.96	100	55
NoGM	NoPCA	TSR	4.94	94	10
GrpGM	PCA	NoGSR	5.6	100	50
IndGM	PCA	NoGSR	5.53	100	53
NoGM	NoPCA	GSR	5.33	94	13
GrpGM	PCA	WMCSF	4.75	95	12
NoGM	PCA	WMCSF	4.2	95	15
IndGM	PCA	WMCSF	4.71	95	13
GrpGM	PCA	GSR	4.82	89	11
GrpGM	PCA	TSR	4.47	92	9
NoGM	PCA	TSR	3.95	92	8
NoGM	PCA	GSR	4.25	92	11
IndGM	PCA	TSR	4.43	92	9
IndGM	PCA	GSR	4.77	90	11

Assessment of residual variance in the extracted time series expectedly reveals that refraining from PCA denoising and using no global signal regression retained more variance. Gray matter masking also seemed to perform well with regard to this measure.

Supplementary analysis

The results of the supplementary analysis conducted using spherical ROIs of 5 mm radius rather than the actual cluster volumes are detailed in the supplementary material. The summary ranking across both indices (Kendall’s correlations and absolute differences) and both perspectives (RoSO and RoCO) of reliability reflect the major patterns noticed in the main analysis, except for the gray matter masking. The supplementary results associated with the PCA denoising and the mean global signal regression remain the same as in the main analysis. In turn, the supplementary results illustrate that using spherical ROI of 5 mm radius (i.e., smaller VOIs) favor No GM masking (cf. Supplementary figure S7).

Discussion

The key idea behind resting-state fMRI analyses is to estimate functional connectivity between distant brain regions based on the correlation of their BOLD time series (Biswal et al. 1995, 1997). The fundamental assumption behind this conceptualization is that the extracted time series reflect the effects of ongoing neuronal computation through hemodynamic coupling, such that correlated signal changes reflect inter-regional synchronization. However, systematic sources of non-neuronal fluctuations in EPI signals likely influence these functional connectivity estimates (Biswal et al. 1995; Friston et al. 1996; Fox and Raichle 2007; Buckner 2010; Cole et al. 2010). Addressing these non-neuronal signals is, therefore, a critical consideration in any functional connectivity approach. In this study, we investigated the influence of various preprocessing approaches meant to deal with this issue, including gray matter masking, PCA denoising, and global signal regression. Our findings are based on investigating two a priori defined networks (the extended socio-affective default mode network and the working-memory network) in a sample of 42 subjects scanned twice, with an average retest-delay of 175 days. We found that gray matter masking based on group-average GM probabilities improved reliability, while confound removal approaches (either PCA denoising or global signal regression) reduced it. However, the study has yielded some mixed results that will be discussed in this section.

AQ3

Recently, Shirer et al. (2015) investigated a confound removal pipeline that optimizes resting state fMRI data, which is comparable to our study. They performed a reliability study dealing with confound removal combined with various bandpass filter selections. In contrast, in this study, the focus is mainly on seed region time-series extraction methods based on different methods for gray-matter masking, combined with various confound removal techniques. There are several additional differences between both studies. Shirer et al. (2015) used ten components for the PCA model (5 from WM and 5 from CSF) and computed WM and CSF signals using a 3-mm radius spherical ROI centered on (arbitrary) WM and CSF regions. In contrast, we here used a five components PCA model, noting that five dominant principle components have been shown to effectively remove the relevant noise (Chai et al. 2012). Moreover, the mean WM and CSF signal was computed using the entire segmented WM and CSF regions in our study, assuming that signal from small regions may not model the appropriate noise term. In addition, they performed reliability analyses to evaluate the motion parameters, whereas we included them in the standard pre-processing given convincing previous evidence for using a 24-parameter motion regression model (Power et al. 2015; Satterthwaite et al. 2013) and bandpass filtered frequencies between 0.01 and 0.08 Hz (Biswal et al. 1995; Cordes et al. 2001; Fox et al. 2005; Zou et al. 2008; Van Dijk et al. 2012; Tsvetanov et al. 2015). Therefore, both studies deal with similar issues but address complementary aspects.

Different perspectives

Reliability of subjects (RoSO) and reliability of connections (RoCO) represent two fundamentally different views on reliability of resting-state measurements (Gorgolewski et al. 2013). Conceptually, assessing the RoSO allows us to identify which combinations of processing steps that yield a reproducible relationship between subjects for each connection, while RoCO identifies the combinations that yield the relationship between different connections in the same subject. RoSO is fundamental for any analysis focusing on between-subject differences. Example applications would include brain-phenotype associations, e.g., the correlation of connectivity estimates with neuropsychological or other behavioral measures (Müller et al. 2014), including clinical analyses comparing patients to healthy control subjects (Zhang and Raichle 2010; Hoptman et al. 2012; Müller et al. 2013). In contrast, RoCO is most relevant when performing any within-subject modeling, either as a primary goal, e.g., when performing connectivity-based parcellation, or to compute derivative measures characterizing the individual connectome (Eickhoff et al. 2011; Bzdok et al. 2013; Clos et al. 2013). Examples of the latter include graph-theory-based analyses that compute characteristic network measures from the individual connectome (Shen et al. 2010; Wang et al. 2011; Reid and Evans 2013). In other words, the results from the RoSO are particularly pertinent, when the focus is on group comparison or across-subject associations, whereas the results from the RoCO are relevant when the focus is on the structure of an individual subject's connectivity matrix.

Assessed (combinations of) signal processing steps

Here, we addressed the effects of gray-matter masking during the ROI time-series extraction (which has received rather little attention up to now), the influence of PCA denoising (which has at times been suggested but is not commonly used), and global signal regression (which is still highly controversial). The extracted ROI time series characterizes the temporal dynamics of the selected region as captured by the evoked BOLD response. While ROI time-series extraction plays a key role when studying the regional specific BOLD signal, the respective methods are rarely discussed even though it may affect reliability of subsequent analyses. For example, gray-matter masking is frequently used to restrict signal extraction to gray matter as much as possible, even though the benefits of doing so have not been explicitly demonstrated. In this study, we thus investigated this issue by examining the reliability of various gray-matter masking approaches.

Probably, the best-investigated source of spurious variance in RS time series is head motion (Van Dijk et al. 2012; Satterthwaite et al. 2013; Griffanti et al. 2014; Patriat et al. 2015; Power et al. 2015; Wong et al. 2016). Satterthwaite et al. (2013), using a 24-parameter motion regression approach, found that the first derivative as well as the quadratic effects of both realignment parameters and derivatives could account for these effects. In addition, in this study, the residual signal after removal of the variance associated with confounds variables is band pass filtered between 0.01 and 0.08 Hz, which is unfortunately known to be influenced by various noise components (Birn et al. 2006). Niazy et al. (2011) indicated that resting-state networks show temporal correlations across a wide frequency range, even though the resting-state networks are dominated by low frequencies of the BOLD signal. However, there is ample evidence that the BOLD signal which is measured by fMRI and from which functional connectivity maps are derived is dominated by low-frequency fluctuations (Biswal et al. 1995; Cordes et al. 2001). Thus, to stay in line with standard applications, we followed the well-established standard of bandpass filtering and motion regression (Satterthwaite et al. 2013). Furthermore, it has been argued that global signal regression may be beneficial to deal with motion effects (Murphy et al. 2009; Power et al. 2012). In contrast, previous studies addressing the influence of global signal removal (Weissenbacher et al. 2009; Chai et al. 2012; Chen et al. 2012) and those assessing test–retest reliability (Shehzad et al. 2009; Gorgolewski et al. 2013; Birn et al. 2014) used less extensive motion regression protocols. Acknowledging new approaches based on automatically classifying and removing noise components have recently emerged (Behzadi et al. 2007), we here focused on three steps commonly used in settings in which physiological noise recording is not available and data quality is not sufficient for reliable estimation of noise components in individual subjects. Therefore, the paper aims to study the reliability and reproducibility of functional connectivity patterns in “clinical quality” data rather than in optimal datasets with low spatial and temporal resolution as well as physiological recordings.

Gray matter masking during time-series extraction

The time series extracted from an ROI represents the time-varying BOLD fluctuations within that region. Using one of the common approaches (Friston et al. 2006), we computed the first eigenvariate to obtain the characteristic time series for each ROI that accounts for the largest proportion of the variance in the set of voxel-wise time series. In general, voxels comprising the ROI may extend into the WM or CSF region, especially for a priori meta-analytically defined clusters, which usually do not respect the tissue class locations of the subjects under study. However, signals obtained from either WM or CSF voxels are not of interest in the functional connectivity analysis, as they should be of non-neuronal origin. One approach to reduce the influence of these unwanted signals and locally optimize the time-series extraction toward the biologically relevant voxels is to use gray matter masking. In that context, however, a fixed threshold for GM segmentation seems inappropriate, given that it could lead to exclusion of entire regions as well as having no effect in others. Our results indicates that using gray-matter masking when extracting the time series, i.e., considering only those voxels in the ROI that are above the median GM probability, yield more reliable connectivity scores.

Since there are no previous investigations into the effect of performing local optimization of ROIs toward gray-matter voxels, we here investigated two different approaches (median split based on the individual and group-averaged

GM probabilities) and compared them to the “baseline” approach of using the entire ROI volume without masking. Factors like head motion could influence the outcome of various GM masks used for time-series extraction investigated in this study. Subjects with higher head motion may benefit either less (due to reduced fit) or more (due to poor individual segmentation) from the group-level GM masking. Therefore, the rationale for evaluating both approaches is that individual GM probabilities should best reflect a particular subject’s anatomy after spatial normalization, but comes at the disadvantage of being potentially noisier given that they are based on a single scan. In contrast, group-level GM probabilities should be less specific but more robust. Our results are particularly true when the mean tissue probabilities across the entire group were used. In our view, this not only indicates the beneficial effects of gray matter masking and hence supports the aforementioned motivation to perform a local optimization, but also suggests that group-level masking, albeit potentially less specific, may be the preferable choice due to increased robustness. In addition, individual GM probabilities produce reliable results for within subject studies. Nevertheless, the segmentations and spatial normalization of the EPI images might be less precise as compared to that of high-resolution T1 images, due to the lower resolution and poorer contrast. This may entail somewhat higher registration inaccuracies, which, in turn, may have had some influence on the results. A straightforward and more traditional approach for gray matter masking would be to use a population-based a priori tissue mask (e.g., ICBM gray matter map). However, the use of such mask to define gray matter in the ROI may be more sensitive to (systematic) registration errors stemming, e.g., from differences in the studied population to the population that was used to construct the a priori tissue masks. In summary, we would thus recommend the use of a study specific group gray matter mask when dealing with large clusters such as derived from neuroimaging meta-analyses.

Interestingly, a somewhat different pattern emerges when representing the regions of interest not by the full highly threshold clusters derived from the meta-analyses (cf. Table 1) but rather by spheres of 5 mm radius around their peak coordinate (cf. Supplementary figures S5–S7). These definitions differ from those used in the main analysis in several aspects. In particular, these spherical ROIs contain a more uniform (compared to the cluster-based ones) and smaller number of voxels. In analyzing the effect of gray matter masking on these spherical ROIs, we found that no masking yielded the best reliability and would propose two possible explanations (cf. Supplementary figures S5–S7). First, the smaller extent of these spherical ROIs most likely yielded a lower proportion of voxels located in WM and CSF, as indicated by a higher mean GM probability, although this is not a criterion for their definition. Second, given the smaller size of the spherical ROIs, the performed median split may have resulted in a critical further reduction of available voxels that renders the results unstable due to session-to-session misalignment, noise, or other factors. As a conclusion, it is advisable to implement gray matter masking for larger, a priori defined clusters based on the group-averaged GM probabilities to improve the reliability. In turn, when using smaller, spherical ROIs, no gray matter masking seems preferable.

PCA denoising

Cleaning the data with PCA denoising has been introduced by Behzadi et al. (2007) and frequently used since (e.g., Kellermann et al. 2013). In this study, we performed PCA denoising using the time course of the five most dominant principal components as confound regressors, effectively removing signal correlated with these. In an evaluation study, Chai et al. (2012) reported that removing principal components derived from WM and CSF regions is advisable to reduce the influence of physiologically induced artifacts, as components derived from WM and CSF regions are unlikely to include neural activity. In particular, it has been argued that physiologically induced artifacts should be particularly present within WM, ventricles, and large vessels (Chang et al. 2009). In addition, PCA denoising should remove effects that are widely distributed over the brain, including again variance related to physiological sources (Chai et al. 2012). Finally, it is worth mentioning that the first principle component is closely related to the global mean signal.

Our results focusing on test–retest reliability from two different perspectives (RoSO and RoCO), however, indicate that PCA denoising is not beneficial under either perspective, irrespectively of the remaining settings. These findings thus replicate the findings by Power et al. (~~2013) (Power et al.~~ 2014) that PCA denoising does not yield encouraging results. In addition, Shirer et al. (2015) observed a decrease in test–retest reliability with PCA denoising. We note that, following the proposed method by Behzadi et al. (2007), the main analysis presented here obtain the principal components from the segmented white matter and CSF masks. As an alternative approach, principle components may also be computed from the whole brain mask, i.e., GM, WM, and CSF. We thus performed an additional analysis using PCA components derived from the entire brain, but observed similar results to those obtained from using WM/CSF derived components (cf. Supplementary figures S8–S10). These results converge with those of Soltysik et al. (2015), which reveal that PCA extracted from whole brain yield similar results to those obtained from using WM and CSF regions. In summary, we would thus argue that PCA denoising has no beneficial effect on the test–retest reliability of RS-FC estimates, at least within the settings evaluated in this study. When investigating resting-state functional connectivity between a priori specified regions of interest refraining from PCA denoising should hence provide the more reliable results.

Global signal regression

Global signal regression, i.e., the removal of variance in the individual voxels' time series that can be explained by the average (global) signal across the entire brain, has become a controversial topic recently. Historically, it was based on the global scaling approaches utilized in the early (functional) PET studies, which were necessary to allow inference on localized and hence specific changes in blood flow. The key idea behind this approach has been retained in virtually all MRI-based neuroimaging studies, rendering global signal regression a common feature for both task- and resting-state fMRI. Similar to its origins in PET, the purpose is again to facilitate the detection of localized neuronal effects. Using GSR assumes that meaningful effects (reflecting activations or functional connectivity) are based on local variations in neuronal activity. Consequently, global signals, which are thought to mainly originate from physiological rather than neuronal sources, should be treated as a confounding influence. In line with this view, Power et al. (2014) observed that global signal regression is also an effective means of reducing motion-related effects in resting-state fMRI data.

Following the outlined logic, global signal removal has been the standard approach for many years until, more recently, it has been argued (Murphy et al. 2009; Weissenbacher et al. 2009; Saad et al. 2012) that GSR might introduce artificial anti-correlations. In addition, Chen et al. (2012) quantified the global noise levels, and based on the noise level within the data set, they advised to determine whether to include or exclude the global signal regressors based on this information. Ultimately, the issue of whether GSR should be employed or not remains contentious. Likewise, the effects of removing global vs. tissue-class specific mean signals, in particular only those for WM and CSF are still unclear. In this study, we thus investigated seven different variants of global signal removal involving global, mean tissue class and mean WM/CSF signal removal at the first or second order as well as no GSR.

Regarding the effects of global signal removal on test–retest reliability, our investigation yields somewhat mixed results. Overall, we found that without any mean signal regression yields the highest reliability over both subjects and connections. However, when looking at the results in more detail, it may be noted that these overall findings are strongly driven by the within-network analyses. Here, not removing any GSR clearly yields the most reliable measures of functional connectivity. In turn, estimates for functional connectivity between the two assessed networks (WMN and eSAD) are most reliable when mean signal time courses for all three-tissue classes were removed from the data. Finally, we noted that removing the mean WM and CSF signal seems to provide a good compromise, as this approach yields reliable estimates of within- and between-network connections, although it is not the best approach in either case. Furthermore, Yan et al. (2013b) suggested that global signal regression is nearly identical to gray matter regression. Thus, both the results from Yan et al. (2013b) and our present data argue for using only the mean WM and CSF signal (but not the mean gray matter) for nuisance signal regression.

The issue of global signal regression is strongly tied to the question of (spurious or induced) anti-correlations. This is also evident in our data. Without any global signal removal, both within- and between-network connections correlate positively. This indicates that global fluctuations override any potential local anti-correlations. Yet, when variance explained by the global signal or the mean WM and CSF is removed, between-network connections become predominantly negative. That is, only when global changes in the BOLD signal are removed, do the estimated functional connectivity values reflect the repeatedly advocated anti-correlated structure of "task-positive" and "task-negative" networks. Should these thus be considered spurious? One argument against this rather critical view comes from task-based fMRI studies (Greicius et al. 2003;

Greicius and Menon 2004), which have clearly shown that regions such as the eSAD reduce their activity during cognitive tasks, which in order recruit fronto-parietal networks such as the working-memory network investigated here. However, global signal removal or, more commonly, scaling is also a standard approach also in task-fMRI (Macey et al. 2004). Another possibility is that global signal may be comprised primarily of non-neuronal sources, rendering the positive correlation between any two parts of the brain in the absence of global signal regression spurious (Murphy et al. 2009). We would, therefore, argue that global (positive) correlation and between-network anti-correlations might be considered as two aspects of a more complex situation. In particular, it seems that anti-correlative structures between large-scale networks are superimposed on larger waves of global signal changes, which may be non-neuronal in origin (Fox et al. 2009). Nevertheless, more recently, Schölvinck et al. (2013) suggested that the global signal is tightly coupled to the neuronal signal. In addition, Pisauro et al. 2016 showed that global components in mice are coupled to pupil dilation as a measure of sympathetic function. Thus, they may be partially neuronal and non-neuronal in origin. In such case, removal of global signals likewise acts as a focus on (smaller) local effects of anti-correlated nature while ignoring the large-scale synchronization of BOLD patterns. In turn, not removing any global signal would preserve the latter and hence bring the positive relation between all time-series that is present in the acquired data into focus.

General discussion

When assessing the test–retest reliability of resting-state fMRI connectivity estimates, one unlikely but still important caveat must be considered. It is possible that increased reliability, i.e., higher correlation and lower absolute difference, will be caused by excessive removal of variance. In the extreme case, when the time series would be reduced to a flat line, test–retest reliability would be perfect. However, ~~also~~ beyond this hypothetical extreme case, the relationship between reliability and variance is interesting; as it sheds light on the question to what extent our methods remove noise (in that case residual variance and reliability would be positively related) or relevant signal (which would render the relationship negative). In our assessment, we found that methods providing results that are more reliable also feature higher residual variance within the extracted time series (Fig. 9, the correlation between residual variance and reliability scores is 0.87) Therefore, reliability seems proportional to the retained variance, reinforcing the observations by Birn et al. (2014) and Yan et al. (2013a).

Another point to consider is the relationship between reliability and validity. The underlying idea of all preprocessing approaches is to remove variance in the data that may be attributable to noise or, more generally, non-neuronal sources. This naively assumes that more aggressive confound removal should increase the biological validity of the obtained results. However, this assumption has been challenged, most notably with respect to global signal regression. Here, it has been argued that removing global signal as a confound may actually introduce a bias in the analysis (Murphy et al. 2009; Weissenbacher et al. 2009; Saad et al. 2012), that may lead to reduction in validity. Conversely, the argument has been made that global signal regression is the most effective approach to remove the effect of motion-related variance (Power et al. 2014) and hence should increase validity. This already illustrates that the relationship between data preprocessing, and in particular confound removal, and validity is not trivial. The present results add another layer of complexity by showing that refraining from using global signal regression and PCA denoising, i.e., using less confounds removal, actually lead to better test–retest reliability. In other words, removing variance that is related to potentially confounding factors reduces reliability, pointing to the possibility that structured noise may be beneficial for test–retest reliability. In addition, indeed, it may be assumed that vascular of physiological factors remain largely stable between sessions and hence help to increase reliability, even though their removal should, in theory, improve the validity of the results. Maximizing (test–retest) reliability and biological specificity/validity may hence represent (partially) conflicting aims.

The functional connectivity strength (i.e., correlation coefficients) between regions might vary with changes in the level of observation noise (Friston 2011). In this study, two resting-state networks (eSAD and WMN), which may be considered as robustly a priori defined resting state networks has been chosen, with prior assumptions such as strong positive coupling among them and anti-correlated with each other (Fox et al. 2005). When there is not any change in the observational noise, then the functional connectivity strength (i.e., correlation coefficients) is expected to be stable (Friston 2011). Therefore, instead of quantifying the connectivity strengths, we mainly focused on reproducibility of the connectivity strength with a certain confound removal within a subject from one session to another session. Furthermore, following the current standard in the field, our study quantified functional connectivity by the Pearson correlations between the time series of two regions. Consequently, other regions within or outside the network could influence such correlations. Such influences, however, were not specifically investigated, given that they should be likewise present in both sessions and, most importantly, the focus of our work is to provide an assessment of how the reproducibility of the widely used time-series correlation measures are based on different approaches to confound removal. That is, we here addressed the pragmatic question, which confound removal strategy yields the highest reliability for a standard analysis approach, rather than addressing which analysis approach may yield the most appropriate representation of a network. Evidently, more investigations are needed to better understand the sources of both noise and signal in resting-state fMRI data, a question that is complicated by a lack of ground truth. Nevertheless, the current results thus point to a potential tradeoff between reliability (which may benefit from structured noise) and biological validity (which should be optimal if all non-neuronal variance is removed (Huettel et al. 2004; Chang et al. 2009; Kim and Ogawa 2012). Based on the present results, we would thus tentatively propose that in cases in which reliability should be of particular importance, for example, in clinical applications, it may be advisable to refrain from global signal regression and PCA denoising to maximize the reliability albeit potentially through the influence of structured noise.

ICA-based denoising is one of the recently emerging confound removal approaches. A recent study showed that it can effectively remove the artifacts coupled with motion (Pruim et al. 2015b) and potential other sources of noise (Griffanti et al. 2014). The entire resting-state scan is decomposed into independent components (IC) (using FSL melodic, http://fsl.fmrib.ox.ac.uk/fsl/fslwiki/MELODIC). ICs coupled with various artifacts were identified with the help of a classifier. ICs classified as noise is then regressed out of the raw fMRI time series. Thus, ICA-based denoising aims to automatically classify and remove the components representing mostly noise rather than neuronal signal (Salimi-Khorshidi et al. 2014; Pruim et al. 2015b). The effectiveness of the strategies mainly depends on the feature selection and the sensitivity of the classifier, as these parameters play a major role in identifying the artifactual signals. In recent evaluation studies, ICA-based denoising strategies resulted in an increase of the between subjects reproducibility (Griffanti et al. 2014; Pruim et al. 2015a). In this study, however, we did not address ICA-based denoising approaches, as we mainly focused on the currently most widely used approaches. In turn, ICA-based denoising is a very promising but yet emerging approach as also demonstrated in our survey. Therefore, further investigations are needed to address the reliability of ICA-based approach both in comparison to and in combination with conventional confound removal strategies. Along with it, there are methods that mainly address local and global artifacts induced by the hardware and partial volume effects (such as: ANATICOR (Jo et al. 2010, 2013)). As th~~is~~e current study mainly studied the influences of biologically induced artifacts, methods like ANATICOR were not addressed here. Furthermore, it has been observed from the literature survey (Fig. 1) that ANATICOR (which has been reported in the categories named 'others') is not a standard method and poorly used in the recent studies.

In this study, the connectivity measures were obtained with standard Pearson correlations. Other approaches have also been applied to this computation, with partial correlation becoming an increasingly advocated alternative (Cole et al. 2010). Partial correlation computes the correlations between two ROIs after regressing out the shared variance of all other ROI time series in the model. However, we are here concerned with testing the effects of several widely used analysis-choices on the reliability of the most common approach. Therefore, given that the overwhelming majority of all resting-state analyses employ full correlations, we here performed a practical evaluation of the impact of currently debated analyses choices on the estimation of functional connectivity by Pearson correlations. Nevertheless, testing the test–retest reliability using partial correlation could be one perspective study of the current one. Furthermore, the subjects were instructed to close their eyes during the resting state session, to reduce the external (visual) stimulation and eye movements. All the subjects included in this study had confirmed to be awake while debriefing. The condition of eyes closed (EC) may be considered as a limitation of the study, as Patriat et al. (2013) showed higher reliability with eyes open (EO) condition rather than eyes closed (EC) condition. However, Patriat et al. (2013)

also reported that the connectivity strengths are not sensitive to the global noise variations. Therefore, further investigations of reliability of EO and EC with and without global noise regression are needed to provide recommendations regarding this parameter. Finally, it has to be noted that the recommendations in this paper may not necessarily apply to brain-behavior analysis examining the relationship between behavioral measures and functional connectivity measures. That is, we here focused on a priori defined meta-analytical networks and their (known) relationships to each other as large-scale anti-correlated systems in the human brain (Fox et al. 2005). What remains to be assessed using a dedicated sample for which test–retest data not only of imaging measures, but also behavioral information is available is this, whether the methods yielding the best reliability in our analysis also provide the most reliable brain-behavior relationships. Likewise, it remains to be tested, whether the identified recommendations also hold for multivariate analyses, e.g., in the context of group classification.

Conclusions

This study assessed test–retest reliability of resting-state fMRI analyses based on a priori ROIs using methods that are applicable without direct recordings of physiological signals (heartbeat, breathing), as is common in clinical and neuroscientific practice. In particular, our results showed that, when using the larger clusters as regions of interest, gray matter masking based on the group-average GM probabilities is advisable. However, In addition, PCA denoising reduces the reliability of connectivity estimates. Finally, with respect to global signal regression, we observed that refraining from this approach enhances test–retest reliability but comes at the expense of potentially poorer biological validity, including missing anti-correlations between what has been previously described as antagonistic networks. Here, removal of global white matter and CSF signals seems to provide a good compromise, as this approach yielded more reliable and potentially meaningful estimates of within- and between-network connections. Importantly, we note that reliability is proportional to the retained variance, presumably including structured noise. Consequently, a compromise exists between maximizing the test–retest reliability and removing variance that may be attributable to non-neuronal sources.

Acknowledgments

This study was supported by the Deutsche Forschungsgemeinschaft (DFG, EI 816/4-1, LA 3071/3-1; EI 816/6-1), the National Institute of Mental Health (R01-MH074457), the Helmholtz Portfolio Theme “Supercomputing and Modeling for the Human Brain” and the European Union Seventh Framework Program (FP7/2007–2013) under Grant Agreement No. 604102 (Human Brain Project).

Compliance with ethical standards

Conflict of interest The authors declare that the research was conducted in the absence of any commercial or financial relationships that could be construed as a potential conflict of interest.

Ethical approval The original study protocol of the data used here has been approved by the local ethics committees of the university hospital Aachen and informed consent was obtained by all the participants prior to the examination. The current data were analyzed anonymously.

Electronic supplementary material

Below is the link to the electronic supplementary material.

Supplementary material 1 (PDF 82383 kb)

References

Amft M, Bzdok D, Laird AR et al (2015) Definition and characterization of an extended social-affective default network. Brain Struct Funct 220:1031–1049. doi:10.1007/s00429-013-0698-0

Ashburner J, Friston KJ (2005) Unified segmentation. Neuroimage 26:839–851. doi:10.1016/j.neuroimage.2005.02.018

Barch DM, Burgess GC, Harms MP et al (2013) Function in the human connectome: task-fMRI and individual differences in behavior. Neuroimage

80:169–189. doi:10.1016/j.neuroimage.2013.05.033

Behzadi Y, Restom K, Liau J, Liu TT (2007) A component based noise correction method (CompCor) for BOLD and perfusion based fMRI. Neuroimage 37:90–101. doi:10.1016/j.neuroimage.2007.04.042

Birn RM, Diamond JB, Smith MABP (2006) Separating respiratory-variation-related fluctuations from neuronal-activity-related fluctuations in fMRI. Neuroimage 31:1536–1548

Birn RM, Molloy EK, Patriat R et al (2013) The effect of scan length on the reliability of resting-state fMRI connectivity estimates. Neuroimage 83:550–558. doi:10.1016/j.neuroimage.2013.05.099

Birn RM, Cornejo MD, Molloy EK et al (2014) The influence of physiological noise correction on test–retest reliability of resting-state functional connectivity. Brain Connect 4:511–522. doi:10.1089/brain.2014.0284

Biswal B, Yetkin FZ, Haughton VM, Hyde JS (1995) Functional connectivity in the motor cortex of resting human brain using echo-planar MRI. Magn Reson Med 34:537–541. doi:10.1002/mrm.1910340409

Buckner RL (2010) Human functional connectivity: new tools, unresolved questions. Proc Natl Acad Sci 107(24):10769–10770

Buckner RL, Bandettini PA, O’Craven KM et al (1996) Detection of cortical activation during averaged single trials of a cognitive task using functional magnetic resonance imaging. Proc Natl Acad Sci USA 93:14878–14883. doi:10.1073/pnas.93.25.14878

Button KS, Ioannidis JPA, Mokrysz C et al (2013a) Power failure: why small sample size undermines the reliability of neuroscience. Nat Rev Neurosci 14:365–376. doi:10.1038/nrn3475

Button KS, Ioannidis JPA, Mokrysz C et al (2013b) Empirical evidence for low reproducibility indicates low pre-study odds. Nat Rev Neurosci 14:877.

doi:10.1038/nrn3475-c6

Bzdok D, Laird AR, Zilles K et al (2013) An investigation of the structural, connectional, and functional subspecialization in the human amygdala. Hum Brain Mapp 34:3247–3266. doi:10.1002/hbm.22138

Chai XJ, Castañón AN, Öngür D, Whitfield-Gabrieli S (2012) Anticorrelations in resting state networks without global signal regression. Neuroimage 59:1420–1428. doi:10.1016/j.neuroimage.2011.08.048

Chang C, Cunningham JP, Glover GH (2009) Influence of heart rate on the BOLD signal: the cardiac response function. Neuroimage 44:857–869. doi:10.1016/j.neuroimage.2008.09.029

Chen G, Chen G, Xie C et al (2012) A method to determine the necessity for global signal regression in resting-state fMRI studies. Magn Reson Med 68:1828–1835. doi:10.1002/mrm.24201

Chen B, Xu T, Zhou C et al (2015) Individual variability and test–retest reliability revealed by ten repeated resting-state brain scans over one month. PLoS One 10:e0144963. doi:10.1371/journal.pone.0144963

Clos M, Amunts K, Laird AR et al (2013) Tackling the multifunctional nature of Broca's region meta-analytically: co-activation-based parcellation of area 44. Neuroimage 83:174–188. doi:10.1016/j.neuroimage.2013.06.041

Cole DM, Smith SM, Beckmann CF (2010) Advances and pitfalls in the analysis and interpretation of resting-state FMRI data. Front Syst Neurosci 4:8. doi:10.3389/fnsys.2010.00008

Cordes D, Haughton VM, Arfanakis K et al (2001) Frequencies contributing to functional connectivity in the cerebral cortex in HResting-state data. Am J Neuroradiol 22:1326–1333

Eickhoff SB, Stephan KE, Mohlberg H et al (2005) A new SPM toolbox for combining probabilistic cytoarchitectonic maps and functional imaging data. Neuroimage 25:1325–1335. doi:10.1016/j.neuroimage.2004.12.034

Eickhoff SB, Laird AR, Grefkes C et al (2009) Coordinate-based activation likelihood estimation meta-analysis of neuroimaging data: a random-effects approach based on empirical estimates of spatial uncertainty. Hum Brain Mapp 30:2907–2926. doi:10.1002/hbm.20718

Eickhoff SB, Bzdok D, Laird AR et al (2011) Co-activation patterns distinguish cortical modules, their connectivity and functional differentiation. Neuroimage 57:938–949. doi:10.1016/j.neuroimage.2011.05.021

Eickhoff SB, Bzdok D, Laird AR et al (2012) Activation likelihood estimation meta-analysis revisited. Neuroimage 59:2349–2361. doi:10.1016/j.neuroimage.2011.09.017

Eickhoff SB, Thirion B, Varoquaux G, Bzdok D (2015) Connectivity-based parcellation: critique and implications. Hum Brain Mapp 36:4771–4792

Fox MD, Raichle ME (2007) Spontaneous fluctuations in brain activity observed with functional magnetic resonance imaging. Nat Rev Neurosci 8:700–711. doi:10.1038/nrn2201

Fox MD, Snyder AZ, Vincent JL et al (2005) The human brain is intrinsically organized into dynamic, anticorrelated functional networks. Proc Natl Acad Sci USA 102:9673–9678. doi:10.1073/pnas.0504136102

Fox MD, Zhang D, Snyder AZ, Raichle ME (2009) The global signal and observed anticorrelated resting state brain networks. J Neurophysiol 101:3270–3283. doi:10.1152/jn.90777.2008

Fox MD, Zhang D, Snyder AZ, Raichle ME (2013) The global signal and observed anticorrelated resting state brain networks 101:3270–3283. doi:10.1152/jn.90777.2008

Fox PT, Lancaster JL, Laird AR, Eickhoff SB (2014) Meta-analysis in human neuroimaging: computational modeling of large-scale databases. Annu Rev Neurosci 37:409–434. doi:10.1146/annurev-neuro-062012-170320

Frässle S, Paulus FM, Krach S, Jansen A (2016) Test–retest reliability of effective connectivity in the face perception network. Hum Brain Mapp 744:730–744. doi:10.1002/hbm.23061

Friston KJ (2011) Functional and effective connectivity: a review. Brain Connect 1:13–36. doi:10.1089/brain.2011.0008

Friston KJ, Williams S, Howard R et al (1996) Movement-related effects in fMRI time-series. Magn Reson Med 35:346–355. doi:10.1002/mrm.1910350312

Friston KJ, Rotshtein P, Geng JJ et al (2006) A critique of functional localisers. Neuroimage 30:1077–1087. doi:10.1016/j.neuroimage.2005.08.012

Gorgolewski KJ, Storkey AJ, Bastin ME et al (2013) Single subject fMRI test–retest reliability metrics and confounding factors. Neuroimage 69:231–243. doi:10.1016/j.neuroimage.2012.10.085

Greicius MD, Menon V (2004) Default-mode activity during a passive sensory task: uncoupled from deactivation but impacting activation. J Cogn Neurosci 16:1484–1492. doi:10.1162/0898929042568532

Greicius MD, Krasnow B, Reiss AL, Menon V (2003) Functional connectivity in the resting brain: a network analysis of the default mode hypothesis. Proc Natl Acad Sci USA 100:253–258. doi:10.1073/pnas.0135058100

Griffanti L, Salimi-Khorshidi G, Beckmann CF et al (2014) ICA-based artefact removal and accelerated fMRI acquisition for improved resting state network imaging. Neuroimage 95:232–247. doi:10.1016/j.neuroimage.2014.03.034

Guo WB, Liu F, Xue ZM et al (2011) Abnormal neural activities in first-episode, treatment-naïve, short-illness-duration, and treatment-response patients with major depressive disorder: a resting-state fMRI study. J Affect Disord 135:326–331. doi:10.1016/j.jad.2011.06.048

He B, Wang Y, Wu D (1999) Estimating cortical potentials from scalp EEG's in a realistically shaped inhomogeneous head model by means of the boundary element method. IEEE Trans Biomed Eng 46:1264–1268. doi:10.1109/10.790505

Hinke RM, Hu X, Stillman AE et al (1993) Functional magnetic resonance imaging of Broca's area during internal speech. NeuroReport 4:675–678

Hoptman MJ, Zuo X-N, D'Angelo D et al (2012) Decreased interhemispheric coordination in schizophrenia: a resting state fMRI study. Schizophr Res 141:1–7. doi:10.1016/j.schres.2012.07.027

Huettel SA, Song AW, McCarthy G (2004) Functional magnetic resonance imaging. Sinauer Associates Publishers, Sunderland

Jo HJ, Saad ZS, Simmons WK et al (2010) Mapping sources of correlation in resting state FMRI, with artifact detection and removal. Neuroimage 52:571–582. doi:10.1016/j.neuroimage.2010.04.246

Jo HJ, Gotts SJ, Reynolds RC et al (2013) Effective preprocessing procedures virtually eliminate distance-dependent motion artifacts in resting state FMRI. J Appl Math. doi:10.1155/2013/935154

Kellermann TS, Caspers S, Fox PT et al (2013) Task- and resting-state functional connectivity of brain regions related to affection and susceptible to concurrent cognitive demand. Neuroimage 72:69–82. doi:10.1016/j.neuroimage.2013.01.046

Kim S-G, Ogawa S (2012) Biophysical and physiological origins of blood oxygenation level-dependent fMRI signals. J Cereb Blood Flow Metab 32:1188–1206. doi:10.1038/jcbfm.2012.23

Kwong KK, Belliveau JW, Chesler DA et al (1992) Dynamic magnetic resonance imaging of human brain activity during primary sensory stimulation. Proc Natl Acad Sci USA 89:5675–5679. doi:10.1073/pnas.89.12.5675

Lai Y, Zhang X, van Drongelen W et al (2011) Noninvasive cortical imaging of epileptiform activities from interictal spikes in pediatric patients. Neuroimage 54:244–252. doi:10.1016/j.neuroimage.2010.07.026

Li Z, Kadivar A, Pluta J et al (2012) Test–retest stability analysis of resting brain activity revealed by blood oxygen level-dependent functional MRI. J Magn Reson Imaging 36:344–354. doi:10.1002/jmri.23670

Lu Y, Worrell GA, Zhang HC et al (2014) Noninvasive imaging of the high frequency brain activity in focal epilepsy patients. IEEE Trans Biomed Eng 61:1660–1667. doi:10.1109/TBME.2013.2297332

Macey PM, Macey KE, Kumar R, Harper RM (2004) A method for removal of global effects from fMRI time series. Neuroimage 22:360–366. doi:10.1016/j.neuroimage.2003.12.042

Müller VI, Cieslik EC, Laird AR et al (2013) Dysregulated left inferior parietal activity in schizophrenia and depression: functional connectivity and characterization. Front Hum Neurosci 7:268. doi:10.3389/fnhum.2013.00268

Müller VI, Langner R, Cieslik EC et al (2014) Interindividual differences in cognitive flexibility: influence of gray matter volume, functional connectivity and trait impulsivity. Brain Struct Funct 220:2401–2414. doi:10.1007/s00429-014-0797-6

Murphy K, Birn RM, Handwerker DA et al (2009) The impact of global signal regression on resting state correlations: are anti-correlated networks introduced? Neuroimage 44:893–905. doi:10.1016/j.neuroimage.2008.09.036

Niazy RK, Xie J, Miller K et al (2011) Spectral characteristics of resting state networks, 1st edn. Elsevier B.V, Amsterdam

Patriat R, Molloy EK, Meier TB et al (2013) The effect of resting condition on resting-state fMRI reliability and consistency: a comparison between resting with eyes open, closed, and fixated. Neuroimage 78:463–473. doi:10.1016/j.neuroimage.2013.04.013

Patriat R, Molloy EK, Birn R (2015) Using edge voxel information to improve motion regression for rs-fMRI connectivity studies. Brain Connect 5:582–595. doi:10.1089/brain.2014.0321

Pisauro MA, Benucci A, Carandini M (2016) Local and global contributions to hemodynamic activity in mouse cortex. J Neurophysiol 115:2931–2936. doi:10.1152/jn.00125.2016

Power JD, Barnes KA, Snyder AZ, Schlaggar BL, Petersen SE (2012) Spurious but systematic correlations in functional connectivity MRI networks arise from subject motion. Neuroimage 59:2142–2154. doi:10.1016/j.neuroimage.2011.10.018.Spurious

Power JD, Mitra A, Laumann TO et al (2014) Methods to detect, characterize, and remove motion artifact in resting state fMRI. Neuroimage 84:320–341. doi:10.1016/j.neuroimage.2013.08.048

Power JD, Schlaggar BL, Petersen SE (2015) Recent progress and outstanding issues in motion correction in resting state fMRI. Neuroimage 105:536–551. doi:10.1016/j.neuroimage.2014.10.044

Pruim RHR, Mennes M, Buitelaar JK, Beckmann CF (2015a) Evaluation of ICA-AROMA and alternative strategies for motion artifact removal in resting state fMRI. Neuroimage 112:278–287. doi:10.1016/j.neuroimage.2015.02.063

Pruim RHR, Mennes M, van Rooij D et al (2015b) ICA-AROMA: a robust ICA-based strategy for removing motion artifacts from fMRI data. Neuroimage 112:267–277. doi:10.1016/j.neuroimage.2015.02.064

Raemaekers M, Du Plessis S, Ramsey NF et al (2012) Test–retest variability underlying fMRI measurements. Neuroimage 60:717–727. doi:10.1016/j.neuroimage.2011.11.061

Reid AT, Evans AC (2013) Structural networks in Alzheimer’s disease. Eur Neuropsychopharmacol 23:63–77. doi:10.1016/j.euroneuro.2012.11.010

Reid AT, Bzdok D, Langner R et al (2016) Multimodal connectivity mapping of the human left anterior and posterior lateral prefrontal cortex. Brain Struct Funct 221:2589–2605

Rottschy C, Langner R, Dogan I et al (2012) Modelling neural correlates of working memory: a coordinate-based meta-analysis. Neuroimage 60:830–846. doi:10.1016/j.neuroimage.2011.11.050

Saad ZS, Gotts SJ, Murphy K et al (2012) Trouble at rest: how correlation patterns and group differences become distorted after global signal regression. Brain Connect 2:25–32. doi:10.1089/brain.2012.0080

Salimi-Khorshidi G, Douaud G, Beckmann CF et al (2014) Automatic denoising of functional MRI data: combining independent component analysis and hierarchical fusion of classifiers. Neuroimage 90:449–468. doi:10.1016/j.neuroimage.2013.11.046

Satterthwaite TD, Elliott MA, Gerraty RT, Ruparel K, Loughead J, Calkins ME, Eickhoff SB, Hakonarson H, Gut RC, Gur REWD (2013) An improved framework for confound regression and filtering for control of motion artifact in the preprocessing of resting-state functional connectivity data. Neuroimage 64:240–256

Schilbach L (2016) Differential patterns of dysconnectivity in mirror neuron and mentalizing networks in schizophrenia. Schizophr Bull. doi:10.1093/schbul/sbw015

Schilbach L, Bzdok D, Timmermans B et al (2012) Introspective minds: using ALE meta-analyses to study commonalities in the neural correlates of emotional processing, social and unconstrained cognition. PLoS One 7:e30920. doi:10.1371/journal.pone.0030920

Schilbach L, Müller VI, Hoffstaedter F et al (2014) Meta-analytically informed network analysis of resting state fMRI reveals hyperconnectivity in an introspective socio-affective network in depression. PLoS One 9:e94973. doi:10.1371/journal.pone.0094973

Schölvinck ML, Leopold DA, Brookes MJ, Khader PH (2013) The contribution of electrophysiology to functional connectivity mapping. Neuroimage 80:297–306. doi:10.1016/j.neuroimage.2013.04.010

Shehzad Z, Kelly AMC, Reiss PT et al (2009) The resting brain: unconstrained yet reliable. Cereb Cortex 19:2209–2229. doi:10.1093/cercor/bhn256

Shen X, Papademetris X, Constable RT (2010) Graph-theory based parcellation of functional subunits in the brain from resting-state fMRI data. Neuroimage 50:1027–1035. doi:10.1016/j.neuroimage.2009.12.119

Shirer WR, Jiang H, Price CM et al (2015) Optimization of rs-fMRI pre-processing for enhanced signal-noise separation, test–retest reliability, and group discrimination. Neuroimage 117:67–79. doi:10.1016/j.neuroimage.2015.05.015

Smith DV, Utevsky AV, Bland AR et al (2014) Characterizing individual differences in functional connectivity using dual-regression and seed-based approaches. Neuroimage 95:1–12. doi:10.1016/j.neuroimage.2014.03.042

Soltysik DA, Thomasson D, Rajan S, Biassou N (2015) Improving the use of principal component analysis to reduce physiological noise and motion artifacts to increase the sensitivity of task-based fMRI. J Neurosci Methods 241:18–29. doi:10.1016/j.jneumeth.2014.11.015

Song X, Lawrence PP, Chen N-K (2016) Data-driven and predefined ROI-based quantification of long-term resting-state fMRI reproducibility. Brain Connect XX:1–16. doi:10.1089/brain.2015.0349

Thomason ME, Dennis EL, Joshi AA et al (2011) Resting-state fMRI can reliably map neural networks in children. Neuroimage 55:165–175. doi:10.1016/j.neuroimage.2010.11.080

Tsvetanov KA, Henson RNA, Tyler LK et al (2015) The effect of ageing on fMRI: correction for the confounding effects of vascular reactivity evaluated by joint fMRI and MEG in 335 adults. Hum Brain Mapp 36:2248–2269.

doi:10.1002/hbm.22768

Van Dijk KR, Sabuncu MR, Buckner RL (2012) The influence of head motion on intrinsic functional connectivity MRI. Neuroimage 59:431–438. doi:10.1016/j.neuroimage.2011.07.044.The

Wang J-H, Zuo X-N, Gohel S et al (2011) Graph theoretical analysis of functional brain networks: test–retest evaluation on short- and long-term resting-state functional MRI data. PLoS One 6:e21976. doi:10.1371/journal.pone.0021976

Weissenbacher A, Kasess C, Gerstl F et al (2009) Correlations and anticorrelations in resting-state functional connectivity MRI: a quantitative comparison of preprocessing strategies. Neuroimage 47:1408–1416. doi:10.1016/j.neuroimage.2009.05.005

Windischberger C, Langenberger H, Sycha T et al (2002) On the origin of respiratory artifacts in BOLD-EPI of the human brain. Magn Reson Imaging 20:575–582. doi:10.1016/S0730-725X(02)00563-5

~~Wise RG, Ide K, Poulin MJTI (2004) Resting fluctuations in arterial carbon dioxide induce significant low frequency variations in BOLD signal. Neuroimage 21:1652–1664~~

AQ4

Wong C-K, Zotev V, Misaki M et al (2016) Automatic EEG-assisted retrospective motion correction for fMRI (aE-REMCOR). Neuroimage 129:133–147. doi:10.1016/j.neuroimage.2016.01.042

Yan CG, Cheung B, Kelly C et al (2013a) A comprehensive assessment of regional variation in the impact of head micromovements on functional connectomics. Neuroimage 76:183–201. doi:10.1016/j.neuroimage.2013.03.004

Yan CG, Craddock RC, Zuo XN et al (2013b) Standardizing the intrinsic brain: towards robust measurement of inter-individual variation in 1000 functional connectomes. Neuroimage 80:246–262.

doi:10.1016/j.neuroimage.2013.04.081

Zang Y, Jiang T, Lu Y et al (2004) Regional homogeneity approach to fMRI data analysis. Neuroimage 22:394–400. doi:10.1016/j.neuroimage.2003.12.030

Zhang D, Raichle ME (2010) Disease and the brains dark energy. Nat Rev Neurol 6:15–28

Zhong S, He Y, Gong G (2015) Convergence and divergence across construction methods for human brain white matter networks: an assessment based on individual differences. Hum Brain Mapp 36:1995–2013. doi:10.1002/hbm.22751

Zou QH, Zhu CZ, Yang Y et al (2008) An improved approach to detection of amplitude of low-frequency fluctuation (ALFF) for resting-state fMRI: fractional ALFF. J Neurosci Methods 172:137–141. doi:10.1016/j.jneumeth.2008.04.012

Zuo XN, Kelly C, Adelstein JS et al (2010) Reliable intrinsic connectivity networks: test–retest evaluation using ICA and dual regression approach. Neuroimage 49:2163–2177. doi:10.1016/j.neuroimage.2009.10.080

Bharat B. Biswal, Joel Van Kylen, James S. Hyde, (1997) Simultaneous assessment of flow and BOLD signals in resting-state functional connectivity maps. NMR in Biomedicine 10 (4-5):165-170